2.5 mg/kg divided on days -3 to -1), and busulfan (4.0 mg/kg/day on days −6 and −5) or melphalan (70 mg/m^2 on days −3 and −2) with or without TBI 3–4 Gy on day 0. The remaining 8 patients received other agents instead of busulfan or melphalan because of chemoresistance. GVHD prophylaxis consisted of tacrolimus and methylprednisolone (mPSL) 1 mg/kg [5]. All patients except 2 received peripheral blood stem cells. T cell depletion was not performed.

Diagnosis of graft-versus-host disease and supportive care

Acute GVHD was graded according to standard criteria [26]. GVHD was treated as previously described [5]. Each patient was isolated in a laminar air-flow room or protective environment room, and standard decontamination procedures were followed. Oral antibiotics (ciprofloxacin, vancomycin, itraconazole or voriconazole) were administered to sterilize the bowel. Patients who were negative for cytomegalovirus (CMV) IgG received blood products from CMV-seronegative donors. Intravenous immunoglobulin was administered at a minimum dose of 100 mg/kg every 2 weeks until day 100. Cotrimoxazole was given for at least 1 year for prophylaxis of *Pneumocystis carinii* infections. Acyclovir was administered at a dose of 1,000 mg/day for 5 weeks after transplantation to prevent herpes simplex virus or varicella-zoster virus infection, and then the agent was continued for at least 2 years at a dose of 200 mg/day. Ganciclovir 7.5 mg/kg divided into 3 doses per day was administered from day −10 to day −3 as prophylaxis for CMV infection.

Measurement of serum sIL-2R

The serum sIL-2R level was monitored from the start of conditioning three times a week until hospital discharge. The serum sIL-2R concentration was evaluated using a commercially available sandwich enzyme-linked immunosorbent assay (ELISA) with two murine anti-human sIL-2R antibodies (CELLFREE Human sIL-2R ELISA Kit; Thermo Fisher Scientific Inc., Rockford, IL, USA). The normal sIL-2R level is <534 U/ml.

Statistics

The background levels of serum sIL-2R were decided using data from 38 patients who did not develop GVHD. The difference in sIL-2R levels on day 7 between patients who developed grade 0–I and grade II–III GVHD was analyzed using the Mann–Whitney U test. In addition, we determined the appropriate cutoff value of the sIL-2R level on day 7 to discriminate patients with and without severe GVHD through receiver operating characteristic (ROC) analysis, in which sensitivity and specificity were calculated as a function of the cutoff value, (1-specificity) was plotted against the sensitivity, and the area under the ROC curve (AUC) was calculated. Cumulative incidence of GVHD for patients with sIL-2R on day 7 of >810 or <810 U/ml was estimated using the Kaplan–Meier method, treating death and relapse as competing risks. Gray's test was used for comparison of cumulative incidence in the 2 groups. To identify factors associated with GVHD, using variables including the donor source, age, disease status before transplantation, sex, number of times of transplantation, HLA disparity in GVH direction, disease, and day 7 sIL-2R level, univariate and multivariate analyses were performed using the Cox proportional hazards model. Results were considered significant when $p \leq 0.05$. Statistical analyses were performed with EZR [27, 28].

Results

Background level of sIL-2R based on the data from patients who did not develop GVHD

Serum sIL-2R levels were monitored 3 times a week to analyze the relationship between sIL-2R levels and the development of GVHD in detail. We first identified the serum background level of sIL-2R based on data from 38 patients who did not develop acute GVHD. As shown in Fig. 1, sIL-2R was slightly high, but mostly <1,200 U/ml during 2 weeks after transplantation, and thereafter slightly decreased to <1,000 U/ml. The median value of sIL-2R

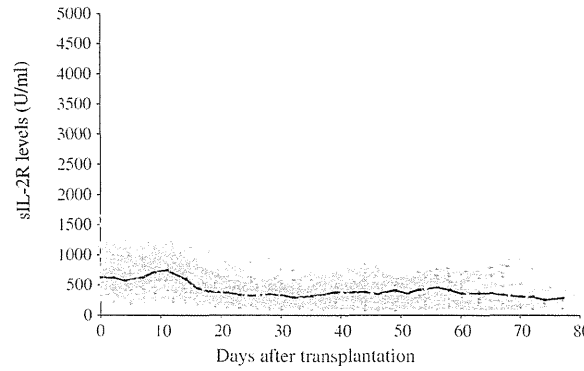

Fig. 1 The kinetics of sIL-2R in patients not developing acute GVHD. To identify the background levels of sIL-2R, changes of serum sIL-2R of 38 patients who did not develop GVHD were plotted. The normal sIL-2R level is <534 U/ml. sIL-2R was slightly high, but mostly <1,200 U/ml during 2 weeks after transplantation, and thereafter slightly decreased to <1,000 U/ml. The *bold line* shows a median sIL-2R level

was slightly increased after transplantation, peaked on day 11 (the peak level was 740 U/ml), and thereafter decreased to levels as low as between 290 and 450 U/ml.

The kinetics of sIL-2R in patients who developed severe GVHD

Next, we analyzed the kinetics of sIL-2R in 25 patients who developed severe (grade II–III) GVHD. Four patients developed skin-only GVHD, 16 gut-only GVHD, and 5 skin/gut GVHD. Those patients developed grade II–III GVHD at a median 28 days (range 3–67 days). The sIL-2R curves were found to vary patient-to-patient in the peak level or in the timing of the peak. The median sIL-2R levels increased after transplantation, reach on day 11 (the peak value of 1,663 U/ml), and thereafter decreased to low levels of <1,000 U/ml after day 30 (Fig. 2).

Regarding the relationship between the kinetics of sIL-2R and the onset of GVHD, 4 patterns were observed. Eight (32 %) patients, in whom sIL-2R increased rapidly after transplantation, developed GVHD at an increasing phase or at the peak level of sIL-2R curve by day 30 (Fig. 3a). These patients developed GVHD at a median of 9 days (range 5–26 days), with the median value of sIL-2R of 1,795 U/ml (range 1,134–4,341 U/ml) at the onset of GVHD. Four (16 %) patients developed GVHD at a decreasing phase of sIL-2R over the peak of sIL-2R (Fig. 3b). These patients developed GVHD at a median of 18.5 days (range 14–21 days), with the median value of sIL-2R of 1,465.5 U/ml (range 618–2,004 U/ml) at the onset of GVHD. Ten (40 %) patients, in whom sIL-2R increased to a high level after transplantation, with the median peak level of 1,711 U/ml (range 1,200–2,977 U/ml) at a median 5.5 days (range 0–16 days), developed GVHD after sIL-2R levels decreased to almost the normal range of sIL-2R (Fig. 3c). These patients developed GVHD at a median of 38 days (range 28–67 days), with the median value of sIL-2R of 642.5 U/ml (range 336–950 U/ml) at the onset of GVHD. Three (12 %) patients, in whom sIL-2R did not increase over the background levels of sIL-2R after transplantation, developed GVHD after day 30, when sIL-2R was slightly increasing over the background level of sIL-2R (Fig. 3d). GVHD in this group of patients occurred latest at a median of 44 days (range 37–59 days), with the median value of sIL-2R of 984 U/ml (range 935–1,054 U/ml) at the onset of GVHD. These results show that GVHD can occur on any point of the sIL-2R curve of patients with GVHD.

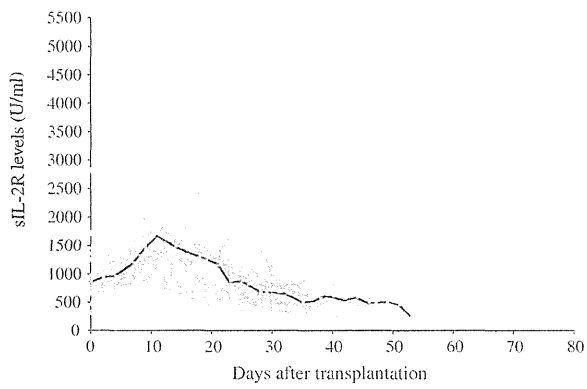

Fig. 2 The kinetics of sIL-2R in 25 patients who developed acute GVHD (grade II–III). Changes of serum sIL-2R in 25 patients who developed severe GVHD were plotted. The sIL-2R curves were found to vary patient-to-patient in the peak level or in the timing of the peak. The *bold line* shows a median sIL-2R level

Prediction of severe acute GVHD by serum sIL-2R levels on day 7

The relationship between sIL-2R change and the onset of GVHD (Fig. 3a–d) shows that the occurrence of GVHD is not limited at the time of high level of sIL-2R or at an increasing phase of sIL-2R; however, the majority of patients who developed severe GVHD showed a high level of sIL-2R early in their transplant course. Therefore, we considered that sIL-2R in the early phase of transplantation may be associated with the development of severe GVHD.

We compared sIL-2R levels on day 7 in patients who developed grade II–III GVHD or grade 0–I GVHD. Consequently, patients with grade II–III GVHD showed significantly higher sIL-2R on day 7 than those with grade 0–I GVHD ($p < 0.0001$). To determine the appropriate cutoff value of sIL-2R on day 7 to discriminate patients with and without severe GVHD, ROC analysis (Fig. 4a) was performed, and the optimal grade II–III GVHD cutoff point was found to be 810 U/ml. The area under the ROC curve (AUC) was 0.790 (CI 0.675–0.904). The relationship between the incidence of severe GVHD and day 7 sIL-2R levels was analyzed using competing risk analysis, treating death and relapse as competing risks. As shown in Fig. 4b, the cumulative incidence of severe GVHD was 43.2 % (CI 28.2–57.3 %) and 6.5 % (CI 1.1–18.9 %) for patients with day 7 sIL-2R >810 U/ml and those with day 7 sIL-2R <810 U/ml, respectively. Patients with day 7 sIL-2R >810 U/ml had a significantly higher risk of GVHD than those with day 7 sIL-2R <810 U/ml ($p = 0.00076$, log-rank test).

Next, using variables including the donor source (offspring vs others), HLA disparity (2 antigen vs 3 antigen) in the GVH direction, older age (>47 years), disease status before transplantation (CR vs non-CR), sex, number of times of transplantation, disease (ALL vs others), and day 7 sIL-2R, factors that were significantly associated with the development of severe GVHD were analyzed using the

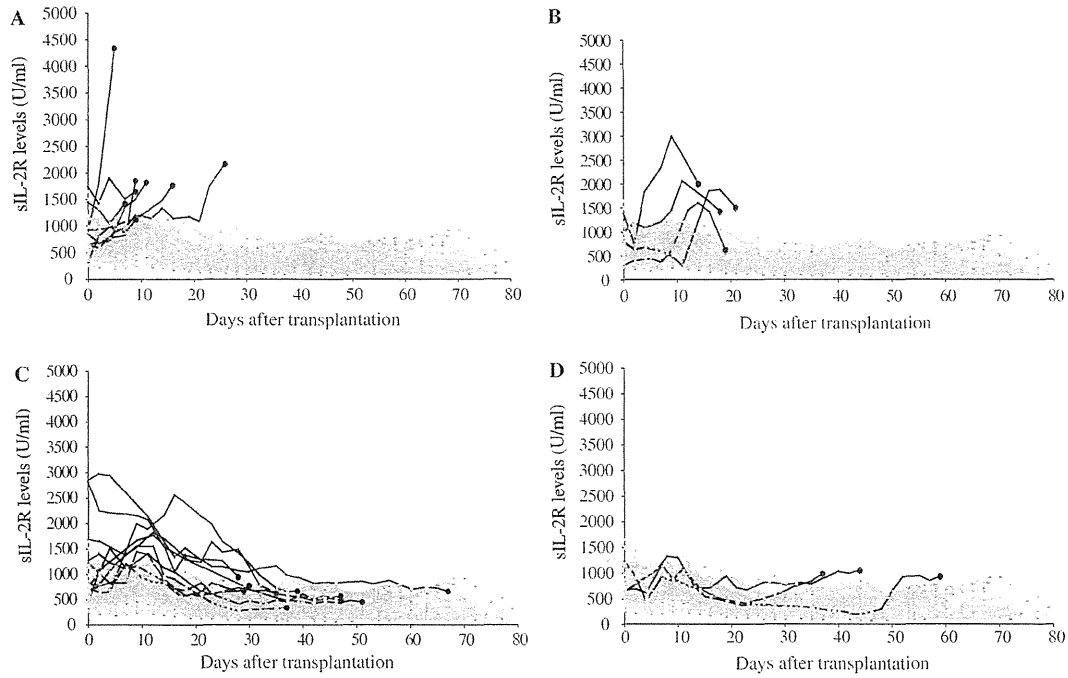

Fig. 3 The relationship between the kinetics of sIL-2R and onset of GVHD in patients who developed severe acute GVHD. *Bold lines* show changes of sIL-2R in patients who developed severe GVHD. *Closed circles*, which are at the end of the *bold lines*, show the onset of GVHD. *Gray lines* show changes of sIL-2R in patients not developing GVHD. **a** GVHD occurred at an increasing phase of sIL-2R or at the peak level by day 30. **b** GVHD occurred at a decreasing phase of sIL-2R (still at a high level) over the peak of sIL-2R. **c** GVHD occurred after returning to the background level of sIL-2R, which passed through the high levels after transplantation. **d** GVHD occurred at a time point slightly increased from the background level of sIL-2R after day 30

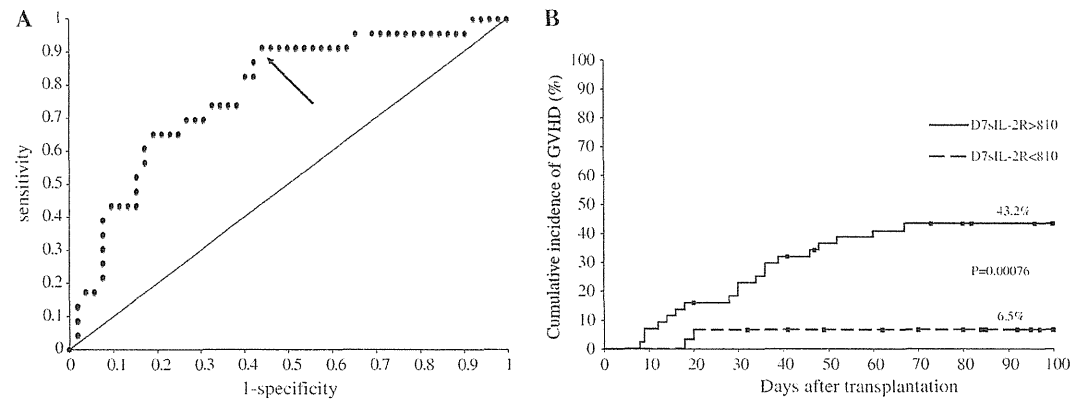

Fig. 4 **a** ROC curve of sIL-2R level on day 7 for the prediction of severe GVHD. To determine the appropriate cutoff value of sIL-2R levels on day 7 to discriminate patients with and without severe GVHD, ROC analysis was performed, and the optimal grade II–III GVHD cutoff point was found to be 810 U/ml, shown by the *arrowhead*. The area under the ROC curve (AUC) was 0.790. **b** Cumulative incidence of severe GVHD for patients with sIL-2R on day 7 of >810 and <810 U/ml. Cumulative incidence of acute GVHD for patients with sIL-2R on day 7 of >810 U/ml and <810 U/ml was estimated using the Kaplan–Meier method, treating death and relapse as competing risks. Gray's test was used for comparison of cumulative incidence in the 2 groups. Patients with sIL-2R on day 7 of >810 U/ml had a significantly higher risk of severe acute GVHD than those with day 7 sIL-2R of <810 U/ml ($p = 0.00076$, log-rank test)

Cox proportional hazards model (Table 2). In a univariate analysis, day 7 sIL-2R >810 U/ml, offspring, age >47 years, and first transplantation were significantly associated with the occurrence of severe GVHD. In a multivariate analysis, day 7 sIL-2R >810 U/ml was only a factor significantly associated with the occurrence of

Table 2 Analysis of factors related to the development of severe GVHD

	Univariate analysis		Multivariate analysis	
	p	CI	*p*	CI
sIL-2R on day 7 (>802 vs <802)	0.0024	2.214–40.431	0.0101	1.597–31.999
Donor source (offspring vs others)	0.0125	1.287–8.102	0.6601	0.238–9.617
Age (>47 vs <47 years)	0.0089	1.389–9.905	0.8337	0.144–11.068
Disease status before transplantation (CR vs non-CR)	0.7203	0.307–5.527	0.1965	0.576–14.591
Sex (female vs male)	0.1877	0.769–3.820	0.526	0.525–3.523
Number of times of transplant (retransplantation vs first transplantation)	0.0155	0.112–0.795	0.2003	0.100–1.621
HLA disparity in GVH direction (2 antigen vs 3 antigen)	0.8831	0.430–2.067	0.5993	0.322–1.922
Disease (ALL vs others)	0.2713	0.152–1.698	0.490	0.181–2.265

CI confidence interval, *CR* complete remission, *non-CR* non-complete remission

severe GVHD ($p = 0.0101$, CI 1.597–31.999). Offspring, age >47 years, and first transplantation had no significant impact on the occurrence of severe GVHD.

Discussion

In the present study, using data from 77 patients who underwent HLA-haploidentical RIST, we investigated the thorough kinetics of serum sIL-2R after transplantation to elucidate the usefulness of sIL-2R as a GVHD biomarker, and found that sIL-2R on day 7 was useful as a predictor of severe GVHD.

In the present study, data from other pathological situations that increase serum sIL-2R were excluded from the analysis. Serum sIL-2R levels reflect the magnitude of the activation and proliferation of T cells, but are not specific to the GVH reaction. This is an inevitable drawback in the diagnosis of GVHD using sIL-2R, as a non-specific T cell reaction of donor or recipient origin produces sIL-2R in some particular transplant complications, such as infection. To avoid the effect of these complications on sIL-2R analysis, other researchers also excluded data from patients with these complications, who represent 15 % of allogeneic recipients [12]. In the present study, a tumor-associated increase in sIL-2R was observed in a slightly high incidence because the majority of patients treated in our institute were in non-CR at the time of transplantation; therefore, data from a slightly higher proportion (20 %) of patients were excluded.

In the absence of GVHD, the median serum sIL-2R was slightly increased after transplantation, peaked on day 11 (the peak level was 740 U/ml), and thereafter decreased to as low as between 290 and 450 U/ml (Fig. 1). On the other hand, in the presence of GVHD, the median serum sIL-2R increased after transplantation, peaked in a median of 11 days (the peak level was 1,663 U/ml), and thereafter decreased to low levels of <600 U/ml (Fig. 2). Compared with the previous studies [14, 16], in which sIL-2R levels peaked 2–3 weeks after transplantation with the peak level of 3,000–5,000 U/ml, sIL-2R in the present study reached the peak level slightly earlier, but the peak levels were lower. The use of ATG-containing RIC regimen and the incorporation of glucocorticoids into the GVHD prophylaxis are considered to contribute to the decrease in the peak level of sIL-2R, which is probably the main reason for a low incidence of severe GVHD observed in our regimen for HLA-haploidentical RIST [5]. Miyamoto et al. [14], in the study of allogeneic SCT using myeloablative conditioning, reported that sIL-2R in patients with GVHD started to increase on day 3, and that the elevation of sIL-2R on day 3 predicted the occurrence of acute GVHD. In the present study, sIL-2R in patients with GVHD started to increase on day 7, as shown in Fig. 2. This discrepancy may be explained by the use of RIC in this study, which induces mixed chimerism status between donor and recipient in the early transplant period, retarding the start of GVH reaction.

The previous studies of sIL-2R only showed that sIL-2R peaked on weeks 2 and 3, or that the peak level of sIL-2R was associated with the severity of GVHD [14, 16]. From the analysis of the onset of GVHD, GVHD was found to occur in 4 different phases of sIL-2R curve: GVHD occurred (1) at an increasing phase or at the peak level of sIL-2R after transplantation (Fig. 3a), (2) at a decreasing phase of sIL-2R (still at a high level) over the peak of sIL-2R (Fig. 3b), (3) after returning to the background level of sIL-2R, which passed through the high levels after transplantation (Fig. 3c), and (4) at a time point slightly increased from the background level of sIL-2R after day 30 (Fig. 3d). Although the prophylactic use of glucocorticoids is considered to contribute to the reduction in sIL-2R levels, as described above, there was no difference among 4 patterns of patients with GVHD in the administration schedule of steroids until the onset of GVHD. The occurrence of GVHD in 4 different phases of sIL-2R curve of

GVHD is not limited to HLA-haploidentical RIST, but observed also in other types of allogeneic SCT, including related HLA- matched, unrelated bone marrow, and umbilical cord blood SCT (data not shown). These results show that GVHD occurs at any time point on the sIL-2R curve, indicating that sIL-2R is not a suitable marker for real-time monitoring of the development of GVHD. Host organ-associated factors [29–31], other than donor T cell activation, must be also associated with the ultimate development of GVHD.

In fact, while sIL-2R peaked at a median of 11 days in patients developing GVHD, GVHD occurred at a median of 28 days. This time lag between the peak level of sIL-2R and the onset of GVHD may be explained as follows. According to the pathophysiology of GVHD that Ferrara et al. [32] proposed, donor T cell activation precedes a series of the subsequent various immunological reactions leading to the development of GVHD. In addition, GVHD may become clinically evident as the dose of immunosuppressive agents is tapered.

On the other hand, the fact that the majority of patients developing GVHD showed a high level of sIL-2R early in their transplant course indicates that sIL-2R levels in the early transplant phase could be a predictor of severe GVHD. In a univariate analysis, day 7 sIL-2R >810 U/ml, offspring, age >47 years, and first transplantation were significantly associated with the occurrence of severe GVHD; however, in a multivariate analysis, day 7 sIL-2R >810 U/ml was only a factor significantly associated with the occurrence of severe GVHD (Table 2). Thus, for the first time, we showed that sIL-2R in the early transplant phase was useful as a GVHD predictor.

The occurrence of events, such as VOD or sepses, until day 7 may result in non-specific increase in sIL-2R on day 7, which make it unable to predict GVHD using day 7 sIL-2R; however, the predictability of GVHD by sIL-2R on day 7 is not basically affected by such pathological events that occur after day 7. Regarding non-specific increase in sIL-2R on day 7, whether we can detect or diagnose such events (inducing increase in sIL-2R) on day 7 is practically important because the GVHD predictor should not be applied if a given patient has such events and shows sIL-2R >810 U/ml. The diagnosis of VOD or severe infections is relatively easy, whereas accurate quantification of residual tumor burden that may lead to tumor-associated increase in sIL-2R may be sometimes difficult. In general, in case of tumor-associated increase, sIL-2R levels are usually high since before transplantation or during conditioning, and tend to gradually or rapidly decrease after transplantation in this early transplant period, whereas, in GVHD-associated increase, sIL-2R levels are increasing at day 7 in most cases, as shown in Fig. 2. Therefore, when applied to patients undergoing allogeneic SCT in CR status, sIL-2R will be more useful as a GVHD predictor. In addition, even if such a non-specific increase blunts the usefulness of sIL-2R as GVHD predictor, when sIL-2R levels are <810 U/ml on day 7, the incidence of GVHD is only 6.5 %, as shown in Fig. 4b, indicating that patients with such low sIL-2R levels have an extremely low risk of developing severe GVHD even in HLA-haploidentical SCT.

In conclusion, in this HLA-haploidentical SCT using the combination of ATG-containing RIC regimen and the incorporation of glucocorticoid into GVHD prophylaxis, sIL-2R levels were mostly suppressed after transplantation compared with other studies on sIL-2R, which possibly lead to a low incidence of severe GVHD. sIL-2R on day 7 was useful as a predictor of GVHD in this transplant setting.

Acknowledgments We thank the medical, nursing, and laboratory staff of the participating departments for their contributions.

Conflict of interest The authors declare no conflict of interest.

References

1. Armitage JO. Medical progress. Bone marrow transplantation. N Engl J Med. 1994;330:827–38.
2. Aversa F, Terenzi A, Tabilio A, Falzetti F, Carotti A, Ballanti S, et al. Full haplotype-mismatched hematopoietic stem-cell transplantation: a phase II study in patients with acute leukemia at high risk of relapse. J Clin Oncol. 2005;23:3447–54.
3. Di Ianni M, Falzetti F, Carotti A, Terenzi A, Castellino F, Bonifacio E, et al. Tregs prevent GVHD and promote immune reconstitution in HLA-haploidentical transplantation. Blood. 2011;117:3921–8.
4. Lu DP, Dong L, Wu T, Huang XJ, Zhang MJ, Han W, et al. Conditioning including antithymocyte globulin followed by unmanipulated HLA-mismatched/haploidentical blood and marrow transplantation can achieve comparable outcomes with HLA-identical sibling transplantation. Blood. 2006;107:3065–73.
5. Ogawa H, Ikegame K, Kaida K, Yoshihara S, Fujioka T, Taniguchi Y, et al. Unmanipulated HLA 2-3 antigen-mismatched (haploidentical) bone marrow transplantation using only pharmacological GVHD prophylaxis. Exp Hematol. 2008;36:1–8.
6. Brunstein CG, Fuchs EJ, Carter SL, Karanes C, Costa LJ, Wu J, et al. Alternative donor transplantation after reduced intensity conditioning: results of parallel phase 2 trials using partially HLA-mismatched related bone marrow or unrelated double umbilical cord blood grafts. Blood. 2011;118:282–8.
7. Lee KH, Lee JH, Lee JH, Kim DY, Seol M, Lee YS, et al. Reduced-intensity conditioning therapy with busulfan, fludarabine, and antithymocyte globulin for HLA-haploidentical hematopoietic cell transplantation in acute leukemia and myelodysplastic syndrome. Blood. 2011;118:2609–17.
8. Diamantstein T, Osawa H. The interleukin-2 receptor, its physiology and a new approach to a selective immunosuppressive therapy by anti-interleukin-2 receptor monoclonal antigen. Immunol Rev. 1986;92:5–27.
9. Minami Y, Kono T, Miyazaki T, Taniguchi T. The IL-2 receptor complex: its structure, function and target genes. Annu Rev Immunol. 1993;11:245–68.

10. Junghans RP, Waldmann TA. Metabolism of Tac (IL2Ralpha): physiology of cell surface shedding and renal catabolism, and suppression of catabolism by antibody binding. J Exp Med. 1996;183:1587–602.
11. Robb RJ, Kutny RM. Structure-function relationships for the IL 2-receptor system. IV. Analysis of the sequence and ligand-binding properties of soluble Tac protein. J Immunol. 1987;139: 855–62.
12. Paczesny S, Krijanovski OI, Braun TM, Choi SW, Clouthier SG, Kuick R, et al. A biomarker panel for acute graft-versus-host disease. Blood. 2009;113:273–8.
13. Siegert W, Josimovic-Alasevic O, Schwerdtfeger R, Baurmann H, Schmidt CA, Musch R, et al. Soluble interleukin-2 receptors in patients after bone marrow transplantation. Bone Marrow Transpl. 1990;6:97–101.
14. Miyamoto T, Akashi K, Hayashi S, Gondo H, Murakawa M, Tanimoto K, et al. Serum concentration of the soluble interleukin-2 receptor for monitoring acute graft-versus-host disease. Bone Marrow Transpl. 1996;17:185–90.
15. Foley R, Couban S, Walker I, Greene K, Chen CS, Messner H, et al. Monitoring soluble interleukin-2 receptor levels in related and unrelated donor allogeneic bone marrow transplantation. Bone Marrow Transpl. 1998;21:769–73.
16. Grimm J, Zeller W, Zander AR. Soluble interleukin-2 receptor serum levels after allogeneic bone marrow transplantation as a marker for GVHD. Bone Marrow Transpl. 1998;21:29–32.
17. Kami M, Matsumura T, Tanaka Y, Mikami Y, Miyakoshi S, Ueyama J, et al. Serum levels of soluble interleukin-2 receptor after bone marrow transplantation: a true marker of acute graft-versus-host disease. Leuk Lymphoma. 2000;38:533–40.
18. Ogawa H, Ikegame K, Soma T, Kawakami M, Tsuboi A, Kim EH, et al. Powerful graft-versus-leukemia effects exerted by HLA-haploidentical grafts engrafted with a reduced-intensity regimen for relapse following myeloablative HLA-matched transplantation. Transplantation. 2004;78:488–9.
19. Ikegame K, Kawakami M, Yamagami T, Maeda H, Onishi K, Taniguchi Y, et al. HLA-haploidentical nonmyeloablative stem cell transplantation: induction to tolerance without passing through mixed chimerism. Clin Lab Haematol. 2005;27:1–3.
20. Lee KH, Lee JH, Lee JH, Kim DY, Kim SH, Shin HJ, et al. Hematopoietic cell transplantation from an HLA-mismatched familial donor is feasible without ex vivo-T cell depletion after reduced-intensity conditioning with busulfan, fludarabine, and antithymocyte globulin. Biol Blood Marrow Transpl. 2009;15: 61–72.
21. Perkins JD, Nelson DL, Rakela J, Grambsch PM, Krom RA, et al. Soluble interleukin-2 receptor level as an indicator of liver allograft rejection. Transplantation. 1989;47:77–81.
22. Kamihira S, Atogami S, Sohda H, Momita S, Yamada Y, Tomonaga M. Significance of soluble interleukin-2 receptor levels for evaluation of the progression of adult T-cell leukemia. Cancer. 1994;73:2753–8.
23. Kalmanti M, Karamolengou K, Dimitriou H, Tosca A, Vlachonikolis I, Peraki M, et al. Serum levels of tumor necrosis factor and soluble interleukin 2 receptor as markers of disease activity and prognosis in childhood leukemia and lymphoma. Int J Hematol. 1993;57:147–52.
24. Pui CH, Ip SH, Iflah S, Behm FG, Grose BH, Dodge RK, et al. Serum interleukin 2 receptor levels in childhood acute lymphoblastic leukemia. Blood. 1988;71:1135–7.
25. Cimino G, Amadori S, Cava MC, De Sanctis V, Petti MC, Di Gregorio AO, et al. Serum interleukin-2 (IL-2), soluble IL-2 receptors and tumor necrosis factor-alfa levels are significantly increased in acute myeloid leukemia patients. Leukemia. 1991;5:32–5.
26. Glucksberg H, Storb R, Fefer A, Buckner CD, Neiman PE, Clift RA, et al. Clinical manifestations of graft-versus-host diseases in human recipients of marrow from HLA matched sibling donors. Transplantation. 1974;18:295–304.
27. Kanda Y. Investigation of the freely available easy-to-use software 'EZR' for medical statistics. Bone Marrow Transpl. 2013;48:452–8.
28. Kanda J, Atsuta Y, Wake A, Ichinohe T, Takanashi M, Morishima Y, et al. Impact of the direction of HLA mismatch on transplantation outcomes in single unrelated cord blood transplantation. Biol Blood Marrow Transpl. 2013;19:247–54.
29. Ferrara JL, Harris AC, Greenson JK, Braun TM, Holler E, Teshima T, et al. Regenerating islet-derived 3-alpha is a biomarker of gastrointestinal graft-versus-host disease. Blood. 2011;118:6702–8.
30. Paczesny S, Braun TM, Levine JE, Hogan J, Crawford J, Coffing B, et al. Elafin is a biomarker of graft-versus-host disease of the skin. Sci Transl Med. 2010;2:13ra2.
31. Paczesny S, Raiker N, Brooks S, Mumaw C. Graft-versus-host disease biomarkers: omics and personalized medicine. Int J Hematol. 2013;98:275–92.
32. Ferrara JL, Levy R, Chao NJ. Pathophysiology mechanism of acute graft-vs.-host disease [review]. Biol Blood Marrow Transpl. 1999;5:347–56.

Granulocyte colony-stimulating factor combined regimen in cord blood transplantation for acute myeloid leukemia: a nationwide retrospective analysis in Japan

Cord blood transplantation (CBT) from an unrelated donor has been increasingly used as an alternative transplant method for adult patients without human leukocyte antigen (HLA)-compatible related or unrelated donors.[1-4] However, the main disadvantage of CBT is still the limited cell dose, especially in adults, and this might contribute to a higher incidence of graft failure and delayed hematopoietic recovery, leading to higher transplant-related mortality (TRM) or overall mortality after CBT.

The purpose of a conditioning regimen prior to allogeneic hematopoietic stem cell transplantation (allo-HSCT) for hematologic malignancies is disease eradication and immunosuppression to overcome graft rejection. Although the standard myeloablative conditioning regimen prior to allo-HSCT has been total body irradiation (TBI) or busulfan combined with cyclophosphamide (CY) for patients with adult acute myeloid leukemia (AML), the role of an intensified conditioning regimen has been analyzed extensively in order to reduce the rate of post-transplant relapse and improve survival.[5-7] However, the majority of these studies analyzed patients receiving allo-HSCT using bone marrow (BM) or mobilized peripheral blood (PB) as a stem cell source. Therefore, an optimal myeloablative conditioning regimen prior to CBT for adult AML still has to be determined.

Granulocyte colony-stimulating factor (G-CSF) stimulates proliferation, differentiation, and functional activation of neutrophils. In clinical use, G-CSF is most commonly used for reducing the duration of neutropenia after chemotherapy and HSCT, and for the mobilization of hematopoietic stem/progenitor cells from the BM into PB

Table 1. Characteristics of patients, cord blood units, and transplantation.

	Total	TBI≥10Gy+Ara-C +CY	TBI≥10Gy+Ara-C /G-CSF+CY	TBI≥10Gy+other	TBI<10Gy+other or non-TBI	P
Number of patients	438	163	80	156	39	
Age						0.61
16-39 years	226(52 %)	74(45 %)	40(50 %)	81(52 %)	17(44 %)	
40-55 years	212(48 %)	89(54 %)	40(50 %)	75(48 %)	22(56 %)	
Sex						0.82
Male	217(50 %)	83(50 %)	42(53 %)	73(47 %)	19(49 %)	
Female	221(50 %)	80(49 %)	38(48 %)	83(56 %)	20(51 %)	
Disease status at CBT *						0.32
Standard risk	214 (49 %)	74(45 %)	45(56 %)	79(51 %)	16(41 %)	
High risk	221(50 %)	87(53 %)	35(44 %)	76(49 %)	23(59 %)	
Unknown	3(<1 %)	2(1 %)	0	1(<1 %)	0	
GVHD prophylaxis						<0.001
Cyclosporine A+methotrexate	304(69 %)	107(66 %)	74(93 %)	100(64 %)	23(59 %)	
Tacrolimus+methotrexate	134(31 %)	56(34 %)	6(8 %)	56(39 %)	16(41 %)	
Number of nucleated cells						0.71
$<2.5\times10^7$/kg	204(47 %)	70(43 %)	40(50 %)	75(48 %)	19(49 %)	
$\geq2.5\times10^7$/kg	200(46 %)	79(48 %)	33(41 %)	70(45 %)	18(37 %)	
Unknown	34(8 %)	14(9 %)	7(9 %)	11(7 %)	2(5 %)	
Number of $CD34^+$cells						0.23
$<1\times10^5$/kg	279(64 %)	110(67 %)	43(54 %)	101(64 %)	25(64 %)	
$\geq1\times10^5$/kg	144(33 %)	52(32 %)	34(43 %)	46(29 %)	12(31 %)	
Unknown	15(3 %)	1(<1 %)	3(4 %)	9(6 %)	2(5 %)	
HLA disparities†						0.24
0	40(9 %)	9(6 %)	7(9 %)	19(1 %)	5(1 %)	
1	148(34 %)	64(39 %)	22(28 %)	50(1 %)	12(1 %)	
≥2	250(57 %)	90(55 %)	51(64 %)	87(1 %)	22(1 %)	
ABO incompatibility						0.11
Match	152(35 %)	67(41 %)	29(36 %)	42(27 %)	14(39 %)	
Major/bidirectional mismatch	175(25 %)	30(18 %)	22(28 %)	47(30 %)	11(28 %)	
Minor mismatch	110(40 %)	66(40 %)	29(36 %)	66(42 %)	14(39 %)	
Unknown	1(<1 %)	0	0	1(<1 %)	0	
Year of CBT						<0.001
1998-2002	56(13 %)	12(7 %)	16(20 %)	24(15 %)	4(10 %)	
2003-2005	158(36 %)	40(25 %)	32(40 %)	64(41 %)	22(56 %)	
2006-2008	224(51 %)	111(68 %)	32(40 %)	68(44 %)	13(33 %)	

Disease status at CBT was classified as standard risk or high risk; complete remission without poor prognostic karyotype according to the MRC10 criteria was classified as standard risk, whereas patients in all other situations were classified as high risk. †The number of HLA disparities was defined as low resolution for HLA-A, -B, and –DR in graft-versus-host direction. Ara-C: cytosine arabinoside; CBT: cord blood transplantation; CY: cyclophosphamide; G-CSF: granulocyte colony-stimulating factor; GvHD: graft-versus-host disease; HLA: human leukocyte antigen; TBI: total body irradiation.

for HSCT. Furthermore, since administration of G-CSF increases the susceptibility to cytarabine arabinoside (Ara-C) through induction of cell cycle entry of dormant leukemia cells,[8,9] the efficacy of concomitant use of G-CSF and chemotherapy has been analyzed.[10,11] Several studies, as well as our own single institute studies, have demonstrated that G-CSF combined with myeloablative conditioning prior to allo-HSCT could be safely and effectively used for patients with myeloid malignancies in a single arm trial.[9,12,13] However, there has been no comparative study of transplant outcomes for AML after allo-HSCT following a conditioning regimen with or without G-CSF. This retrospective study is the first to assess the effect of a G-CSF combination in a myeloablative conditioning regimen for CBT on the transplant outcome in adult AML patients in Japan. Patients and study methods are described in the *Online Supplementary Appendix*.

Characteristics of patients and cord blood units are shown in Table 1. There was a significant difference in cumulative incidence of neutrophil recovery among the four groups in univariate analysis (P<0.001) (Figure 1A). In the multivariate analysis, the hazard risk of neutrophil engraftment was significantly higher in the TBI≥10Gy+Ara-C/G-CSF+CY group (P<0.001) and lower in the TBI≥10Gy+other group (P=0.03) and TBI<10Gy+other or non-TBI group (P<0.001) compared with the TBI≥10Gy+Ara-C+CY group (Table 2). Among patients achieving neutrophil engraftment, neutrophil recovery times were significantly shorter in the TBI≥10Gy+Ara-C/G-CSF+CY group compared with the TBI≥10Gy+Ara-C+CY group (P<0.001). There was a significant difference in cumulative incidence of platelet recovery among the four groups in univariate analysis (P<0.001) (Figure 1B). Multivariate analysis showed no significant difference between the TBI≥10Gy+Ara-C+CY group and TBI≥10Gy+Ara-C/G-CSF+CY group (P=0.14). However, the hazard risk of platelet engraftment was significantly lower in the TBI≥10Gy+other group (P<0.001) and TBI<10Gy+other or non-TBI group (P<0.001) compared with the TBI≥10Gy+Ara-C+CY group (Table 2). Among patients achieving platelet engraftment, there was no significant difference in platelet recovery times among the four groups (P=0.32).

Among patients in the entire cohort, the cumulative incidence of TRM at 100 days and at one year was 17% (95%CI: 13%-20%) and 22% (95%CI: 18%-26%), respectively. There was no significant difference in cumulative incidence of TRM at one year among the four groups in univariate analysis (P=0.19) (Figure 1C). Multivariate analysis of TRM, adjusting for other variables, showed no significant difference between the TBI≥10Gy+Ara-C+CY group and the TBI≥10Gy+Ara-C/G-CSF+CY group (P=0.67), TBI≥10Gy+other group (P=0.25), or TBI<10Gy+other or non-TBI group (P=0.95) (Table 2). The cumulative incidence of relapse at three years was 30% (95%CI: 25%-35%) in the entire cohort. There was no significant difference in cumulative incidence of relapse at three years among the four groups (P=0.05) (Figure 1D). In multivariate analysis, the hazard risk of relapse was lower in the TBI≥10Gy+Ara-C/G-CSF+CY group (P=0.03), but not in the TBI≥10Gy+other group (P=0.94) and TBI<10Gy+other or non-TBI group (P=0.73) compared with the TBI≥10Gy+Ara-C+CY group (Table 2).

Among the entire cohort, the probability of disease-free survival (DFS) and overall survival (OS) at three years was 44% (95%CI: 39%-49%) and 52% (95%CI: 46%-57%), respectively. There was a significant difference in the probability of DFS at three years among the four groups in univariate analysis (P=0.001) (Figure 1E). The probability of

Table 2. Multivariate analysis of transplant outcomes.

Outcomes	N. of patients	HR (95 % CI)	P
Neutrophil engraftment			
Conditioning regimen			
TBI≥10Gy+Ara-C+CY	163	1	Reference
TBI≥10Gy+Ara-C/G-CSF+CY	80	1.57(1.17-2.11)	0.002
TBI≥10Gy+other	156	0.76(0.58-0.98)	0.03
TBI<10Gy+other or non-TBI	39	0.46(0.27-0.78)	0.004
Number of CD34$^+$cells			
<1×10^5/kg	279	1	Reference
≥1×10^5/kg	144	1.56(1.23-1.98)	<0.001
Platelet engraftment			
Conditioning regimen			
TBI≥10Gy+Ara-C+CY	163	1	Reference
TBI≥10Gy+Ara-C/G-CSF+CY	80	1.25(0.92-1.71)	0.14
TBI≥10Gy+other	156	0.54(0.39-0.73)	<0.001
TBI<10Gy+other or non-TBI	39	0.40(0.23-0.67)	<0.001
Number of CD34$^+$cells			
<1×10^5/kg	279	1	Reference
≥1×10^5/kg	144	1.58(1.22-2.06)	<0.001
Transplant-related mortality			
Conditioning regimen			
TBI≥10Gy+Ara-C+CY	163	1	Reference
TBI≥10Gy+Ara-C/G-CSF+CY	80	0.86(0.44-1.68)	0.67
TBI≥10Gy+other	156	1.31(0.82-2.10)	0.25
TBI<10Gy+other or non-TBI	39	1.02(0.46-2.25)	0.95
Age			
<40 years	226	1	Reference
≥40 years	212	1.64(1.08-2.49)	0.01
Disease status at CBT			
Standard risk	214	1	Reference
High risk	221	1.81(1.20-2.72)	0.004
Relapse			
Conditioning regimen			
TBI≥10Gy+Ara-C+CY	163	1	Reference
TBI≥10Gy+Ara-C/G-CSF+CY	80	0.45(0.21-0.95)	0.03
TBI≥10Gy+other	156	0.98(0.61-1.57)	0.94
TBI<10Gy+other or non-TBI	39	1.14(0.53-2.44)	0.73
Disease status at CBT			
Standard risk	214	1	Reference
High risk	221	3.28(2.16-4.98)	<0.001
Treatment failure			
Conditioning regimen			
TBI≥10Gy+Ara-C+CY	163	1	Reference
TBI≥10Gy+Ara-C/G-CSF+CY	80	0.57(0.36-0.91)	0.01
TBI≥10Gy+other	156	1.24(0.90-1.70)	0.17
TBI<10Gy+other or non-TBI	39	1.24(0.75-2.02)	0.39
Disease status at CBT			
Standard risk	214	1	Reference
High risk	221	3.10(2.29-4.19)	<0.001
Overall mortality			
Conditioning regimen			
TBI≥10Gy+Ara-C+CY	163	1	Reference
TBI≥10Gy+Ara-C/G-CSF+CY	80	0.52(0.31-0.87)	0.01
TBI≥10Gy+other	156	1.19(0.84-1.69)	0.31
TBI<10Gy+other or non-TBI	39	1.25(0.74-2.12)	0.39
Disease status at CBT			
Standard risk	214	1	Reference
High risk	221	2.68(1.93-3.71)	<0.001

The only significant variables other than conditioning regimen were described in each end point. Variables considered in multivariate analysis were conditioning regimen (TBI≥10Gy+Ara-C+CY vs. TBI≥10Gy+Ara-C/G-CSF+CY vs. TBI≥10Gy+other vs. TBI<10Gy+other or non-TBI), age (<40 vs. ≥40 years), patients' gender (male vs. female), disease status at CBT (standard risk vs. high risk), GVHD prophylaxis (cyclosporine A with methotrexate vs. tacrolimus with methotrexate), cord blood nucleated cell count (<2.5×10^7/kg vs. ≥2.5×10^7/kg), cord blood CD34$^+$ cell count (<1×10^5/kg vs. ≥1×10^5/kg), HLA disparities (0 vs. 1 vs. ≥2), donor–recipient ABO compatibility (match vs. major/bidirectional mismatch vs. minor mismatch), and year of CBT (1998-2002 vs. 2003-2005 vs. 2006-2008). Ara-C: cytosine arabinoside; CBT: cord blood transplantation; CI: confidence interval; CY: cyclophosphamide; G-CSF: granulocyte colony-stimulating factor; HR: hazard ratio; TBI: total body irradiation.

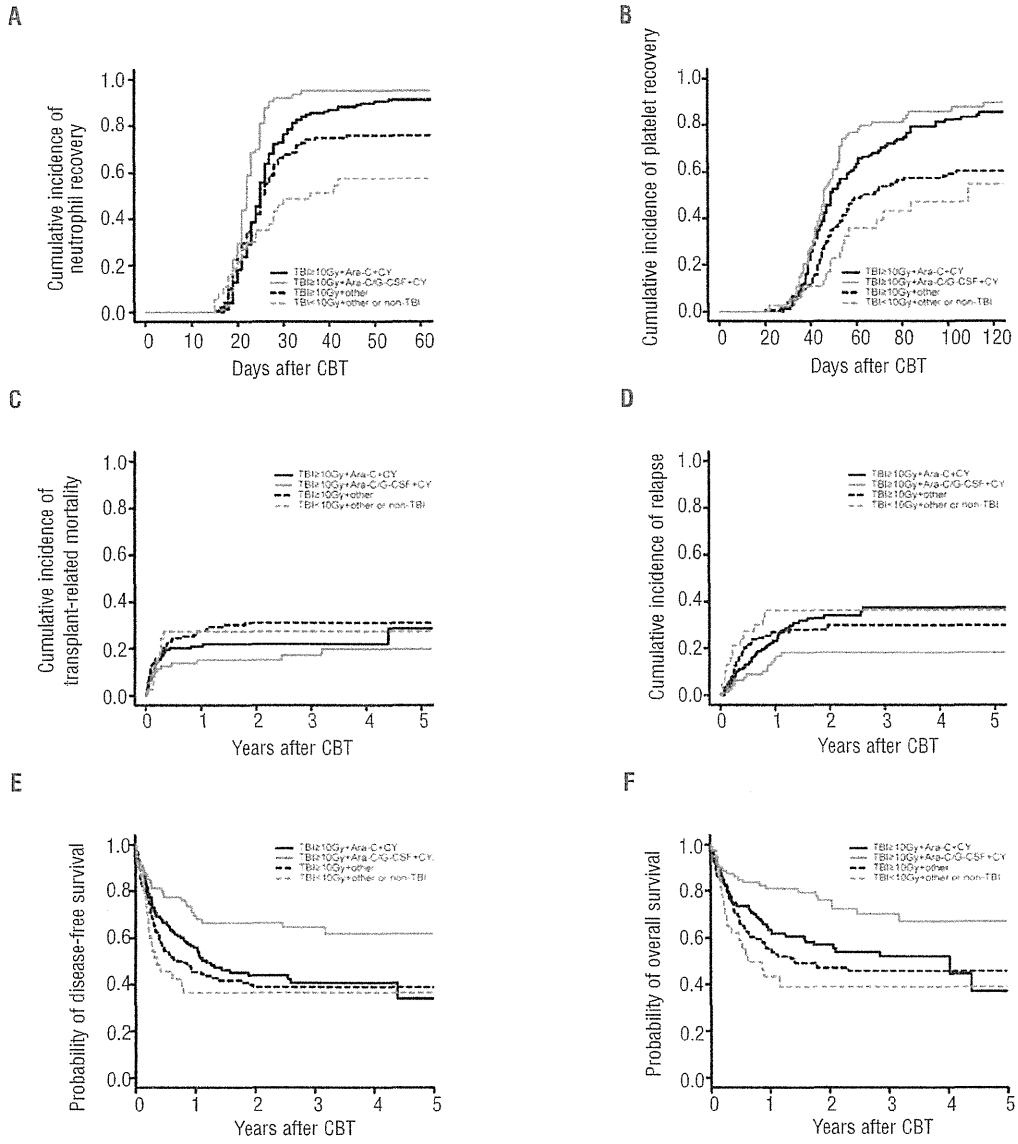

Figure 1. Cumulative incidences of neutrophil (A) and platelet (B) recovery, transplant-related mortality (TRM) (C) and relapse (D), probabilities of disease-free survival (E) and overall survival (F) after cord blood transplantation according to conditioning regimen. (A) Cumulative incidence of neutrophil recovery 42 days after CBT was 88% [95% confidence interval (CI): 81%-92%] in the TBI≥10Gy+Ara-C+CY group, 95% (95%CI: 85%-98%) in the TBI≥10Gy+Ara-C/G-CSF+CY group, 74% (95%CI: 66%-81%) in the TBI≥10Gy+other group, and 57% (95%CI: 37%-70%) in the TBI<10Gy+other or non-TBI group. Median times to neutrophil recovery were 24 days (range 17-53 days) in the TBI≥10Gy+Ara-C+CY group, 22 days (range 16-34 days) in the TBI≥10Gy+Ara-C/G-CSF+CY group, 23 days (range 15-65 days) in the TBI≥10Gy+other group, and 22 days (range 15-42 days) in the TBI<10Gy+other or non-TBI group. (B) Cumulative incidence of platelet recovery 100 days after CBT was 82% (95%CI: 74%-87%) in the TBI≥10Gy+Ara-C+CY group, 85% (95%CI: 74%-92%) in the TBI≥10Gy+Ara-C/G-CSF+CY group, 58% (95%CI: 48%-66%) in the TBI≥10Gy+other group, and 47% (95%CI: 25%-62%) in the TBI<10Gy+other or non-TBI group. Median times to platelet recovery were 46 days (range 28-168 days) in the TBI≥10Gy+Ara-C+CY group, 45.5 days (range 27-263 days) in the TBI≥10Gy+Ara-C/G-CSF+CY group, 48 days (range 20-249 days) in the TBI≥10Gy+other group, and 51 days (range 22-109 days) in the TBI<10Gy+other or non-TBI group. (C) Cumulative incidence of TRM at one year was 21% (95%CI: 15%-27%) in the TBI≥10Gy+Ara-C+CY group, 15% (95%CI: 8%-23%) in the TBI≥10Gy+Ara-C/G-CSF+CY group, 27% (95%CI: 20%-35%) in the TBI≥10Gy+other group, and 27% (95%CI: 14%-42%) in the TBI<10Gy+other or non-TBI group. (D) Cumulative incidence of relapse at three years was 37% (95%CI: 28%-46%) in the TBI≥10Gy+Ara-C+CY group, 18% (95%CI: 10%-27%) in the TBI≥10Gy+Ara-C/G-CSF+CY group, 30% (95%CI: 22%-37%) in the TBI≥10Gy+other group, and 36% (95%CI: 20%-52%) in the TBI<10Gy+other or non-TBI group. (E) Probability of disease-free survival at three years was 40% (95%CI: 31%-49%) for the TBI≥10Gy+Ara-C+CY group, 64% (95%CI: 52-74%) for the TBI≥10Gy+Ara-C/G-CSF+CY group, 38% (95%CI: 30%-47%) for the TBI≥10Gy+other group, and 36% (95%CI: 20%-51%) for the TBI<10Gy+other or non-TBI group. (F) Probability of overall survival was 52% (95%CI: 42%-60%) for the TBI≥10Gy+Ara-C+CY group, 70% (95%CI: 57%-79%) for the TBI≥10Gy+Ara-C/G-CSF+CY group, 45% (95%CI: 36%-54%) for the TBI≥10Gy+other group, and 39% (95%CI: 22%-55%) for the TBI<10Gy+other or non-TBI group. Median period of follow up for survivors (n=261) in the entire cohort was 24 months (range 1-122 months) after CBT.

DFS at three years was significantly better in the TBI≥10Gy+Ara-C/G-CSF+CY group compared with the TBI≥10Gy+Ara-C+CY group (P=0.02), the TBI≥10Gy+other group (P=0.002) and TBI<10Gy+other or non-TBI group (P=0.006). Multivariate analysis showed significantly decreased rates of treatment failure in the TBI≥10Gy+Ara-C/G-CSF+CY group compared with the TBI≥10Gy+Ara-C+CY group (P=0.01) (Table 2). In univariate analysis, there was a significant difference in the probability of OS at three years among the four groups (P=0.001) (Figure 1F). Multivariate analysis showed significantly decreased overall mortality in the TBI≥10Gy+Ara-C/G-CSF+CY group compared with the TBI≥10Gy+Ara-C+CY group (P=0.01) (Table 2). We also analyzed a subgroup of patients with standard risk (n=214) or high risk (n=221) at CBT. In standard-risk patients, the hazard risk of overall mortality (P=0.04), treatment failure (P=0.01) and relapse (P=0.002) was significantly lower in the TBI≥10Gy+Ara-C/G-CSF+CY group compared with the TBI≥10Gy+Ara-C+CY group, while that of high-risk patients was not (*Online Supplementary Table S1 and Figures S1 and S2*).

Anti-leukemia effects of allo-HSCT consist of leukemia eradication by both a conditioning regimen of chemotherapy with or without radiation and the graft-versus-leukemia (GvL) effect. Since relapse is the most common cause of death after allo-HSCT, an intensified conditioning regimen or enhancement of GvL effects is needed to reduce the incidence of relapse. Because of the difficulty in controlling the degree of GvL effects, an intensified conditioning regimen has been extensively analyzed. The several improvements to a typical conditioning regimen have included the addition of other agents to a standard myeloablative regimen, a dose escalation of drugs or TBI, or administration of drugs other than CY. Among these, the addition of other agents to a standard myeloablative regimen has been the most commonly used.[5,6] In fact, several studies have reported a decrease in the incidence of relapse following intensified conditioning, but with a higher TRM, and no improvement in survival was achieved.[5,7] Furthermore, the effect of adding high-dose Ara-C to a TBI/CY myeloablative conditioning regimen is controversial.[7] However, all of these studies analyzed patients receiving BM or mobilized PB stem cell transplantation from related or unrelated donors. This finding was not confirmed in CBT. In our study, neutrophil and platelet engraftment was significantly higher in the TBI≥10Gy+Ara-C+CY group compared with the TBI≥10Gy+other group, suggesting that the addition of Ara-C to TBI/CY was beneficial in terms of stable engraftment, but not for survival in CBT for AML.

Granulocyte colony-stimulating factor was originally identified as an agent for stimulation of neutrophil production. Although G-CSF is most commonly used to reduce the duration of neutropenia after chemotherapy, it is also commonly used for hematopoietic stem cell (HSC) mobilization for HSCT. Although the mechanism of HSC mobilization is not clearly understood, G-CSF could disrupt the contact between HSC in a BM niche, leading to HSC migration. In a mouse bone marrow transplantation (BMT) model, G-CSF prior to low-dose irradiation enhanced donor HSC engraftment.[14] This effect might be mainly due to the migration of recipient HSC from a BM niche by G-CSF treatment before transplantation. In fact, our data showed that neutrophil engraftment was significantly higher in the TBI≥10Gy+Ara-C/G-CSF+CY group compared with the TBI≥10Gy+Ara-C+CY group. These data suggest that the effect of the addition of G-CSF to a conditioning regimen could enhance neutrophil engraftment after CBT.

It has been reported that the administration of G-CSF increased the susceptibility of the cell-cycle-specific agent Ara-C in leukemia cells *in vitro* and in a xenograft model.[8,9,15] In clinical studies, several regimens have attempted to demonstrate the efficacy of concomitant use of G-CSF with chemotherapy for newly diagnosed AML.[10,11] We hypothesized that the addition of G-CSF to a conditioning regimen might improve outcome in an allo-HSCT setting. In our study, relapse was significantly lower in the TBI≥10Gy+Ara-C/G-CSF+CY group compared with the TBI≥10Gy+Ara-C+CY group. In a subgroup analysis, the effect of a G-CSF combination regimen for reduced relapse was significant in standard-risk but not high-risk patients. This is similar to a previous prospective randomized study of concomitant use of G-CSF with chemotherapy by Löwenberg *et al.*[11] Further studies are required to confirm which subgroup of patients with AML could benefit from a G-CSF combination regimen in CBT to reduce the incidence of relapse.

In conclusion, our data show that the addition of G-CSF-combined Ara-C to a TBI+CY conditioning regimen resulted in a significantly higher incidence of neutrophil engraftment and significantly better DFS and OS, and a reduced relapse rate in CBT for AML. Although these findings should be confirmed in prospective studies, a G-CSF-combined myeloablative conditioning regimen promotes better engraftment and survival results in CBT for AML.

Takaaki Konuma,[1] Jun Ooi,[2] Naoyuki Uchida,[3] Hiroyasu Ogawa,[4] Kazuteru Ohashi,[5] Heiwa Kanamori,[6] Nobuyuki Aotsuka,[7] Yasushi Onishi,[8] Hiroki Yamaguchi,[9] Yasuji Kozai,[10] Tokiko Nagamura-Inoue,[11] Koji Kato,[12] Ritsuro Suzuki,[13] Yoshiko Atsuta,[14,15] Seiko Kato,[1] Shigetaka Asano,[16] and Satoshi Takahashi[17]

[1]Department of Hematology and Oncology, The Institute of Medical Science, The University of Tokyo; [2]Department of Hematology and Oncology, Teikyo University School of Medicine, Tokyo; [3]Department of Hematology, Toranomon Hospital, Tokyo; [4]Division of Hematology, Department of Internal Medicine, Hyogo College of Medicine, Nishinomiya; [5]Hematology Division, Tokyo Metropolitan Cancer and Infectious Diseases Center, Komagome Hospital, Tokyo; [6]Department of Hematology, Kanagawa Cancer Center, Yokohama; [7]Division of Hematology-Oncology, Japanese Red Cross Society Narita Hospital, Narita, Japan; [8]Department of Hematology and Rheumatology, Tohoku University Hospital, Sendai; [9]Department of Hematology, Nippon Medical School, Tokyo; [10]Department of Transfusion Medicine, Tokyo Metropolitan Tama Medical Center, Tokyo; [11]Department of Cell Processing and Transfusion, Research Hospital, The Institute of Medical Science, The University of Tokyo; [12]Department of Hematology and Oncology, Children's Medical Center, Japanese Red Cross Nagoya First Hospital; [13]Department of HSCT Data Management and Biostatistics, Nagoya University Graduate School of Medicine; [14]Japanese Data Center for Hematopoietic Cell Transplantation, Nagoya; [15]Nagoya University Graduate School of Medicine; [16]System Medical Biology Laboratory, School of Advanced Science and Engineering, Waseda University, Tokyo; and [17]Division of Molecular Therapy, The Advanced Clinical Research Center, The Institute of Medical Science, The University of Tokyo, Japan

Correspondence: tkonuma@ims.u-tokyo.ac.jp

doi:10.3324/haematol.2014.114504

Key words: cord blood transplantation, conditioning regimen, granu-

locyte colony-stimulating factor, acute myeloid leukemia

Information on authorship, contributions, and financial & other disclosures was provided by the authors and is available with the online version of this article at www.haematologica.org.

References

1. Takahashi S, Iseki T, Ooi J, Tomonari A, Takasugi K, Shimohakamada Y, et al. Single-institute comparative analysis of unrelated bone marrow transplantation and cord blood transplantation for adult patients with hematologic malignancies. Blood. 2004; 104(12):3813-20.
2. Takahashi S, Ooi J, Tomonari A, Konuma T, Tsukada N, Oiwa-Monna M, et al. Comparative single-institute analysis of cord blood transplantation from unrelated donors with bone marrow or peripheral blood stem-cell transplants from related donors in adult patients with hematologic malignancies after myeloablative conditioning regimen. Blood. 2007;109(3):1322-30.
3. Atsuta Y, Suzuki R, Nagamura-Inoue T, Taniguchi S, Takahashi S, Kai S, et al. Disease-specific analyses of unrelated cord blood transplantation compared with unrelated bone marrow transplantation in adult patients with acute leukemia. Blood. 2009;113(8):1631-8.
4. Eapen M, Rocha V, Sanz G, Scaradavou A, Zhang MJ, Arcese W, et al. Effect of graft source on unrelated donor haemopoietic stem-cell transplantation in adults with acute leukaemia: a retrospective analysis. Lancet Oncol. 2010;11(7):653-60.
5. Kanda Y, Sakamaki H, Sao H, Okamoto S, Kodera Y, Tanosaki R, et al. Effect of conditioning regimen on the outcome of bone marrow transplantation from an unrelated donor. Biol Blood Marrow Transplant. 2005;11(11):881-9.
6. Mengarelli A, Iori A, Guglielmi C, Romano A, Cerretti R, Torromeo C, et al. Standard versus alternative myeloablative conditioning regimens in allogeneic hematopoietic stem cell transplantation for high-risk acute leukemia. Haematologica. 2002;87(1):52-8.
7. Riddell S, Appelbaum FR, Buckner CD, Stewart P, Clift R, Sanders J, et al. High-dose cytarabine and total body irradiation with or without cyclophosphamide as a preparative regimen for marrow transplantation for acute leukemia. J Clin Oncol. 1988;6(4):576-82.
8. Miyauchi J, Kelleher CA, Wang C, Minkin S, McCulloch EA. Growth factors influence the sensitivity of leukemic stem cells to cytosine arabinoside in culture. Blood. 1989;73(5):1272-8.
9. Takahashi S, Okamoto SI, Shirafuji N, Ikebuchi K, Tani K, Shimane M, et al. Recombinant human glycosylated granulocyte colony-stimulating factor (rhG-CSF)-combined regimen for allogeneic bone marrow transplantation in refractory acute myeloid leukemia. Bone Marrow Transplant. 1994;13(3):289-45.
10. Pabst T, Vellenga E, van Putten W, Schouten HC, Graux C, Vekemans MC, et al. Favorable effect of priming with granulocyte colony-stimulating factor in remission induction of acute myeloid leukemia restricted to dose escalation of cytarabine. Blood. 2012; 119(23):5367-73.
11. Löwenberg B, van Putten W, Theobald M, Gmür J, Verdonck L, Sonneveld P, et al. Effect of priming with granulocyte colony-stimulating factor on the outcome of chemotherapy for acute myeloid leukemia. N Engl J Med. 2003;349(8):743-52.
12. Mori T, Tanaka M, Kobayashi T, Ohashi K, Fujisawa S, Yokota A, et al. Prospective multicenter study of single-unit cord blood transplantation with myeloablative conditioning for adult patients with high-risk hematologic malignancies. Biol Blood Marrow Transplant. 2013;19(3):486-91.
13. Konuma T, Kato S, Ooi J, Oiwa-Monna M, Ebihara Y, Mochizuki S, et al. Single-unit cord blood transplantation after granulocyte colony-stimulating factor-combined myeloablative conditioning for myeloid malignancies not in remission. Biol Blood Marrow Transplant. 2014; 20(3):396-401.
14. Mardiney M 3rd, Malech HL. Enhanced engraftment of hematopoietic progenitor cells in mice treated with granulocyte colony-stimulating factor before low-dose irradiation: implications for gene therapy. Blood. 1996;87(10):4049-56.
15. Saito Y, Uchida N, Tanaka S, Suzuki N, Tomizawa-Murasawa M, Sone A, et al. Induction of cell cycle entry eliminates human leukemia stem cells in a mouse model of AML. Nat Biotechnol. 2010; 28(3):275-80.

STEM CELLS®

TISSUE-SPECIFIC STEM CELLS

Prospectively Isolated Human Bone marRow Cell-Derived MSCs Support Primitive Human CD34-Negative Hematopoietic Stem Cells

Yoshikazu Matsuoka[1], Ryusuke Nakatsuka[1], Keisuke Sumide[1], Hiroshi Kawamura[1,2], Masaya Takahashi[3], Tatsuya Fujioka[1], Yasushi Uemura[4], Hiroaki Asano[5], Yutaka Sasaki[1], Masami Inoue[6], Hiroyasu Ogawa[7], Takayuki Takahashi[8], Masayuki Hino[9], and Yoshiaki Sonoda[1]

[1]Department of Stem Cell Biology and Regenerative Medicine, Graduate School of Medical Science; [2]Department of Orthopedic Surgery; [3]Department of Pediatrics, Kansai Medical University, Hirakata, Osaka, Japan; [4]Division of Cancer Immunotherapy, Exploratory Oncology Research and Clinical Trial Center, National Cancer Center, Kashiwa, Chiba, Japan; [5]School of Nursing, Kyoto Prefectural University of Medicine, Kyoto, Kyoto, Japan; [6]Department of Hematology/Oncology, Osaka Medical Center and Research Institute for Maternal and Child Health, Izumi, Osaka, Japan; [7]Division of Hematology, Department of Internal Medicine, Hyogo College of Medicine, Nishinomiya, Hyogo, Japan; [8]Department of Hematology, Shinko Hospital, Kobe, Hyogo, Japan; [9]Department of Hematology, Graduate School of Medicine, Osaka City University, Osaka, Osaka, Japan.

Address for correspondence: Yoshiaki Sonoda, M.D., Ph.D., [1]Department of Stem Cell Biology and Regenerative Medicine, Graduate School of Medical Science, Kansai Medical University, 2-5-1 Shinmachi, Hirakata, Osaka 573-1010, Japan; Phone: +81-72-804-2391 Fax: +81-72-804-2399 e-mail: sonoda@hirakata.kmu.ac.jp; Disclosure of Potential Conflict of Interest: The authors declare no potential conflicts of interest

Received July 16, 2014; accepted for publication December 07, 2014;

1066-5099/2014/$30.00/0

This article has been accepted for publication and undergone full peer review but has not been through the copyediting, typesetting, pagination and proofreading process which may lead to differences between this version and the Version of Record. Please cite this article as doi: 10.1002/stem.1941

Key words. MSC • CD271 • SSEA-4 • CD34-negative • HSC • niche

ABSTRACT

Hematopoietic stem cells (HSCs) are maintained in a specialized bone marrow (BM) niche, which consists of osteoblasts, endothelial cells and a variety of mesenchymal stem/stromal cells (MSCs). However, precisely what types of MSCs support human HSCs in the BM remain to be elucidated because of their heterogeneity. In this study, we succeeded in prospectively isolating/establishing three types of MSCs from human BM-derived lineage- and CD45-negative cells, according to their cell surface expression of CD271 and stage-specific embryonic antigen (SSEA)-4. Among them, the MSCs established from the Lineage$^-$CD45$^-$CD271$^+$SSEA-4$^+$ fraction (DP MSC) could differentiate into osteoblasts and chondrocytes, but they lacked adipogenic differentiation potential. The DP MSCs expressed significantly higher levels of well-characterized HSC-supportive genes, including IGF-2, Wnt3a, Jagged1, TGFβ3, nestin, CXCL12, and Foxc1, compared with other MSCs. Interestingly, these osteo-chondrogenic DP MSCs possessed the ability to support cord blood-derived primitive human CD34-negative severe combined immunodeficiency (SCID)-repopulating cells. The HSC-supportive actions of DP MSCs were partially carried out by soluble factors, including IGF-2, Wnt3a and Jagged1. Moreover, contact between DP MSCs and CD34-positive (CD34$^+$) as well as CD34-negative (CD34$^-$) HSCs was important for the support/maintenance of the CD34$^{+/-}$ HSCs *in vitro*. These data suggest that DP MSCs might play an important role in the maintenance of human primitive HSCs in the BM niche. Therefore, the establishment of DP MSCs provides a new tool for the elucidation of the human HSC/niche interaction *in vitro* as well as *in vivo*. STEM CELLS *2014; 00:000–000*

INTRODUCTION

Hematopoietic stem cells (HSCs) are thought to be maintained in the bone marrow (BM) microenvironment, also referred to as the HSC niche [1, 2]. The HSC niche controls the self-renewal, cell cycle, proliferation and differentiation of HSCs. A number of recent studies have revealed that these niches consisted of osteoblasts [3, 4], endothelial cells [5, 6], perivascular cells [6], CXCL12 abundant reticular (CAR) cells [7, 8] and nestin-positive or negative mesenchymal stem cells (MSCs) [9, 10]. However, these niche components were mainly discovered from mouse studies, hence, it has not been

clarified whether these cells also function as unique components of the HSC niche in human BM.

The MSCs are components of BM cells, and are enriched in the BM mononuclear cell (MNC) fraction [11]. The MSCs are plastic-adherent cells that have the capacity to form fibroblast colony-forming unit (CFU-F) and they are distinguished by their in vitro trilineage differentiation into adipogenic, chondrogenic and osteogenic cells. These MSCs are also called mesenchymal "stromal" cells, because their stemness (self-renewal and multilineage differentiation capacity) has still not yet been fully elucidated. Moreover, the cellular origin of the MSCs also remains unclear [12].

Interestingly, it was reported that cultured human MSCs contain three types of clones, which possessed osteo-chondro-adipogenic, osteo-chondrogenic and only osteogenic differentiation capacity [13]. It was also reported that human MSCs expressed CD29, CD44, CD73, CD90, CD105 and STRO-1 [14-17]. Importantly, almost all of these results were obtained from cultured MSCs. A number of investigators have addressed the prospective isolation of primary MSCs from human BM cells. They reported that CD146 [16], CD271 [14, 17, 18] and the combination of these two markers [19], stage-specific embryonic antigen (SSEA)-4 [20], monoclonal antibodies (mAbs) against human mesenchymal stem cell antigen-1 (MSCA-1) [21] and the combination of PDGFRα and CD51 [22] were useful markers for the prospective isolation of primary human MSCs. However, precisely which types of MSCs support primitive human HSCs in the BM niche remain to be elucidated.

Lifelong blood cell production is supported by rare HSCs which possess self-renewal capacity and are able to replenish mature hematopoietic cells via a series of lineage-restricted hematopoietic progenitor cells (HPCs) [23-25]. The human primitive HSCs can be measured based on the severe combined immunodeficiency (SCID)-repopulating cell (SRC) activity using a murine xenograft model [26-28]. The surface immunophenotypes of most primitive human HSCs have been believed to be lineage marker-negative (Lin^-) CD34-positive ($CD34^+$), and CD38-negative ($CD38^-$) [27-29]. However, we have recently demonstrated that the CD34-negative ($CD34^-$) SRCs also exist in human cord blood (CB) [30]. The $CD34^-$ SRC activity is detected only by intra-bone marrow injection (IBMI) [30]. Meanwhile, the $CD34^-$ SRCs could produce $CD34^+$ SRCs both *in vitro* and *in vivo* [30, 31], and $CD34^-$ and $CD34^+CD38^-$ SRCs exhibit almost equivalent abilities for long-term repopulation [32-34]. These results suggest that $CD34^-$ SRCs are more immature than $CD34^+CD38^-$ SRCs [35].

In the present study, in order to investigate what types of MSCs possess the ability to support primitive human HSCs, different subtypes of MSCs were prospectively isolated from human BM. For this purpose, we subdivided a Lin^-CD45^- cell fraction of human BM MNCs according to the surface expression levels of CD271 and SSEA-4. As a result, we succeeded to establish three types of MSCs. The MSCs established from the CD271 and SSEA-4 double-positive fraction (DP MSC) could differentiate into osteoblasts and chondrocytes, but they lacked adipogenic differentiation potential. Interestingly, the DP MSCs, which expressed significantly higher levels of well-characterized HSC- supportive genes, including CXCL12 and FOXC1 [36], showed a higher level of $CD34^-$ SRC-supportive ability. These data demonstrated, for the first time, that prospectively isolated osteo-chondrogenic DP MSCs possess the ability to support very primitive $CD34^-$ SRCs and they might contribute to HSC maintenance in the human BM niche.

MATERIALS AND METHODS

Establishment of human BM-derived MSCs

Immunomagnetically enriched Lin^- BM cells were stained with fluorescein isothiocyanate (FITC)-conjugated 11 Lin-specific mAbs, against CD2, CD16, CD24 and CD235a (DAKO, Kyoto, Japan), CD3, CD41 and CD66c (Beckman Coulter, Fullerton, CA), CD4 and CD14 (eBioscience, San Diego, CA), CD19 and CD56 (BD Biosciences, San Jose, CA), and with an anti-CD45-PacificBlue (PB) mAb (BioLegend, San Diego, CA), anti-CD271-Phycoerythrin (PE) mAb (BD Biosciences), anti-SSEA-4-Apophycocyanin (APC) mAb (R&D Systems, Minneapolis, MN) and 7-aminoactinomycin D (AAD) (Beckman Coulter). Then, $7\text{-}AAD^-Lin^-CD45^-$ cells were subdivided into four fractions according to their expression levels of CD271 and SSEA-4, and these cells were sorted using a FACSAria (BD Biosciences) or FACSAria III (BD Biosciences), as shown in Figure 1.

The collected cells were cultured in α-modified minimum essential medium (α-MEM: Nakalai Tesque, Kyoto, Japan) plus 10% fetal calf serum (FCS) (BioWest, Kansas City, MO) in T-75 culture flasks (BD Biosciences) at 37 ºC, in a fully humidified atmosphere with 5% CO_2. The culture medium was replaced with fresh medium twice a week. Adherent cells were subcultured when cells were reached approximately 80 % confluent, and cells were washed twice with Ca^{2+}- and Mg^{2+}-free phosphate-buffered saline (PBS^-) (Nakalai Tesque), dissociated using 0.25 % Trypsin-EDTA (Life Technologies, Gaithersburg, MD) and split 1:4 into new culture flasks. At the third passage, cells were stored using Cell Banker (Juji Field, Tokyo, Japan) in the -80ºC refrigerator until use. The details information about the antibodies is listed in the Table S1. We also established MSCs from unfractionated BM MNCs using the same methods as those employed for the control. For the clonal analysis of single BM $Lin^-CD45^-CD271^+SSEA\text{-}4^+$ cell-derived MSCs, the assay conditions have slight modifications, as described in the supplemental data.

Analysis of the differentiation potentials of established BM-MSCs

To assess the differentiation capacities of established MSCs, the cells were respectively cultured in osteogenic, adipogenic and chondrogenic differentiation media

at the passage 4, using the Human Mesenchymal Stem Cell Functional Identification Kit (R&D systems) according to the manufacturer's instructions. The non-induced groups were cultured in differentiation media without the supplements as controls. After 21 days of cultures, the cells were fixed by 4% paraformaldehyde, and then reacted with primary Abs against osteocalcin (1:200, R&D systems), fatty acid binding protein 4 (FABP4, 1:200, R&D systems) and aggrecan (1:200, R&D systems). The negative controls were incubated without primary Abs. The primary Abs were visualized by goat anti-mouse IgG conjugated with Alexa Flour 488 (1:200, Life Technologies) or donkey anti-goat IgG conjugated with Alexa Flour 546 (1:200, Life Technologies). The nuclei were stained with Hoechst 33342 (Life Technologies). The fluorescent images were observed by using fluorescent microscopy (BX-50, Olympus, Tokyo, Japan), and were recorded with a cooled CCD camera and the IP Lab Spectrum software package. Osteogenic and adipogenic differentiation were also confirmed by Alizarin red S (Sigma-Aldrich, Tokyo, Japan) and Oil red O (Sigma-Aldrich) staining, respectively.

Coculture of 18Lin⁻CD34$^{+/-}$ cells with established BM-MSCs

Each type of established MSC at passage 4 was seeded on 12-well culture plates (BD Biosciences) seven days before starting cocultures. When the MSCs were reached confluence, the cells were irradiated (12 Gy using a ^{137}Cs-γ irradiator). As we reported previously [33], the sorted 18Lin⁻CD34^{+} (0.5 x 10^4 cells per well) and 18Lin⁻CD34⁻ cells (1.5 x 10^4 cells per well), which contain highly purified human SRCs, were seeded onto MSC feeders and cocultured for one week in StemPro34 serum-free medium (Life Technologies) in the presence of a cocktail of cytokines, including 50 ng/mL stem cell factor (SCF) (BioScience Autogen, Wiltshire, UK), 50 ng/mL flt3 ligand (FL) (R&D Systems), 100 ng/mL thrombopoietin (TPO), 10 ng/mL interleukin (IL)-3 (R&D Systems), 100 U/mL IL-6 (kindly provided by Ajinomoto Co. Inc., Tokyo, Japan) and 10 ng/mL granulocyte colony-stimulating factor (G-CSF) under 5% CO_2, 5% O_2 and 90% N_2 at 37°C. G-CSF and TPO were kindly provided by Kyowa Kirin Company (Tokyo, Japan). After the culture, all of the cells were collected by vigorous pipetting, and then, cells were processed for further analysis.

SRC assay

Six-week-old female NOD/Shi-scid/IL-2Rγ$_c^{null}$ (NOG) mice were purchased from the Central Institute for Experimental Animals (Kawasaki, Japan). All mice were handled under sterile conditions and were maintained in germ-free isolators located in the Central Laboratory Animal Facilities of Kansai Medical University. The animal experiments were approved by the Animal Care Committees of Kansai Medical University. The cocultured 18Lin⁻CD34⁻ cells were collected and resuspended in α-MEM. The cells collected from each set of triplicate cocultures were mixed. Then, two out of nine portions of the collected cells were directly injected into the left tibiae of irradiated (2.5 Gy using a ^{137}Cs-γ irradiator) eight-week-old NOG mice (n=4/group) using our IBMI method [30-34]. The remaining cells were used for cell counting and the FCM analyses. The mice were sacrificed 20 weeks after transplantation, and the murine BM in the left tibia (left tibia) and right tibia, right and left femurs (other bones), thymus and peripheral blood were respectively collected. Then, the multilineage differentiation potentials of the transplanted SRCs were confirmed by FCM as reported previously [30-34]. All of the collected mouse samples were treated with BD PharmLyse (BD Biosciences) before the FCM analyses, except for those used to detect CD235a- and CD41-positive cells in the BM.

Statistical analysis

In Figures 5, 6, S3, S4, S7 and S8, the differences between each pair of the all means were examined by the Tukey's multi comparison procedure. In Table S2, the differences in the lineage differentiation potentials of the cocultured 18Lin⁻CD34$^{+/-}$ cells were examined by the main effect of the factor on the lineage differentiation potentials in a two-way analysis of variance without any confounding effects. Differences were considered significant at a confidence level <0.05.

RESULTS

Isolation of human BM-derived Lin⁻CD45⁻ CD271$^{+/-}$SSEA-4$^{+/-}$ cells

As shown in Figure 1, the human BM-derived Lin⁻CD45⁻ cells were further subdivided into CD271⁻SSEA-4^{+} (SSEA-4 single-positive; SSEA-4 SP, R5), CD271^{+}SSEA-4^{+} (double-positive; DP, R6), CD271⁻SSEA-4⁻ (double-negative; DN, R7) and CD271^{+}SSEA-4⁻ (CD271 single-positive; CD271 SP, R8) fractions (Figure 1E) according to their expression levels of CD271 and SSEA-4. The fractionated cells were sorted and collected for subsequent experiments.

Establishment of human BM-derived mesenchymal stem/stromal cells (MSCs)

Next, we observed the morphologies of the subdivided BM-derived Lin⁻CD45⁻ cells (Figure S1). The size of freshly isolated SSEA-4 SP cells (15-20 μm) (Figure S1A) was larger than that of the DP (Figure S1B) and CD271 SP (Figure S1C) cells, and these cells showed relatively homogenous appearances. However, the cells in the DN fraction contained small and large blastoid cells (Figure S1D).

To test the CFU-F abilities of these four fractions, the sub-fractionated cells were cultured on the plastic culture dishes. We found that the frequency of CFU-F was the highest in the DP fraction (approximately 1/6, Figure 2B). On the other hand, the frequencies of CFU-F in the CD271 SP, SSEA-4 SP and DN fractions were 1/264,

1/84,231 and 1/13,766, respectively (Figures 2A, C, D). We could not establish MSCs from the SSEA-4 SP fraction because of their low CFU-F activity. All of these adherent cells had basically spindle-shaped morphologies in vitro (Figures 2E-G). However, the MSCs established from the DN fraction (DN MSC) had a higher forward scatter level compared with other MSCs (Figure 2H) and showed a polygonal shape (Figure 2F). These MSCs could be cultured for at least one hundred days or more than 10 passages. As shown in Figure 2I, all of the MSCs showed logarithmic growth curves during this culture period.

Next, we analyzed the cell surface marker expression of established MSCs. All of the MSCs expressed CD29, CD44, CD73, CD90 and CD105 (Figure 3A). These markers were already reported to be expressed on MSCs [17, 19, 21]. In addition, these MSCs also expressed HLA-ABC, but not HLA-DR. On the contrary, none of these MSCs expressed the endothelial cell marker, CD31, or hematopoietic cell markers, including CD34, CD41, CD45 and CD56 (Figure 3A). The expression levels of CD271 on the MSCs established from the DP and CD271 SP fractions were down-regulated during *in vitro* passages as shown in Figure 3B. In contrast, the expression of SSEA-4 was upregulated under the culture conditions even in the MSCs established from the DN fraction. Therefore, the surface immunophenotypes of these MSCs were indistinguishable after the culture.

Osteogenic, adipogenic and chondrogenic differentiation potentials of established MSCs

Next, we assessed the differentiation potentials of these three established MSCs. The MSCs (passage 4) were induced to differentiate into osteogenic (Figure 4, top and second rows), adipogenic (Figure 4, center and fourth rows) and chondrogenic (Figure 4, bottom row) lineages. We found that the MSCs derived from the unfractionated BM MNC, DN and CD271 SP fractions could differentiate into all three lineages. Interestingly, the DP MSCs could also be induced to differentiate into osteoblasts and chondrocytes, but most DP MSCs could not differentiate into adipocytes (Figure 4, center and fourth rows). Therefore, these established MSCs had similar morphologies and immunophenotypes, however, they had disparate differentiation potentials *in vitro*.

The gene expression profiles of the three established MSCs

Next, we analyzed the differences in the gene expression profiles among these three established MSCs. We examined the expression patterns of the hematopoietic-supportive genes that had already been reported to be expressed in the mouse or human HSC niche cells by quantitative reverse-transcription PCR (qRT-PCR). In addition, genes essential for mesenchymal lineage differentiation were also examined (Figure 5). The data clearly showed that the expression levels of hematopoietic-supportive genes, including *IGF2*, *WNT3A*, *JAG1*, *ANGPT1*, *TGFB3*, *CXCL12* and *FOXC1*, were significantly higher in the DP MSCs than in the other MSCs.

The DP MSCs expressed significantly higher levels of osteogenic genes (*RUNX2* and *SP7*) than did the DN MSCs or CD271 SP MSCs. On the other hand, the CD271 SP MSCs expressed a significantly higher level of an osteo-chondrogenic differentiation gene (*SOX9*) compared with the DN MSCs. However, a gene associated with adipogenic differentiation, *PPARG*, could not be detected in any of these MSCs in the steady state (data not shown). The expression level of the nestin gene (*NES*), which was expressed in some mouse and human MSCs [9, 22, 37], in the DP MSCs was approximately three-fold higher than that in the CD271 SP and DN MSCs ($p<0.01$). Interestingly, the DP MSCs expressed a significantly higher level of *FOXC1*, which was demonstrated to be essential for CAR cell development in the mouse BM [36], compared with the other MSCs. In contrast, the expression level of *CDH2*, which was expressed in murine osteoblastic niche cells [1, 4], in the DP MSCs was significantly lower than that in the unfractionated BM MNC-derived and CD271 SP MSCs.

MSCs support the human cord blood-derived primitive CD34⁻ HSCs

In order to elucidate whether human BM-derived MSCs support HSCs in the human BM niche similar to the function of mouse MSCs, the $CD34^{+/-}$ HPCs/HSCs-supportive abilities of the three established MSCs were first assessed using a coculture system. The MSCs were seeded and cultured for seven days before starting the coculture. Eighteen $Lin^-CD34^{+/-}$ cells were isolated from CB MNCs by FACS, as reported previously [33]. We confirmed that $18Lin^-CD34^-$ cell fractions were not contaminated by $CD34^+$ cells by post-sort analysis (Figure S2). Then, $18Lin^-CD34^{+/-}$ cells were cultured with or without feeder MSCs for seven days in the presence of a cocktail of cytokines. After the cocultures, the cells were collected, and the supportive abilities of the MSCs for HPCs/HSCs were assessed by cell proliferation/differentiation assays *in vitro* as well as an *in vivo* SRC assay.

In the cocultures of $18Lin^-CD34^+$ cells, the numbers of cells were increased approximately 390 to 550-fold, but the numbers of cells expanded were not significantly influenced from the presence of the MSC feeder cells compared with stroma-free culture (Figure S3A left panel, $p>0.05$). On the other hands, the DP (75-fold $p<0.05$) and CD271 SP MSCs (70-fold, $p<0.01$) significantly suppressed the growth of $18Lin^-CD34^-$ cells compared with the stroma-free control (130-fold) (Figure S3A right panel). The percentages of $CD34^+$ cells after seven days cocultures of $18Lin^-CD34^{+/-}$ cells with DP MSCs (39% and 30%, $p<0.01$) and CD271 SP MSCs (37% and 26%, $p<0.01$) were significantly higher than those of stroma-free controls (14% and 9%) (Figure S3B). On the contrary, the percentage of $CD34^+$ cells in the coculture of $18Lin^-CD34^-$ cells with DN MSCs (3%, $p<0.01$) was significantly lower than that in the stroma-free control.

In addition, the DP MSCs maintained or generated significantly higher numbers of $CD34^+$ cells from $18Lin^-CD34^{+/-}$ cells (18.2×10^4 and 2.3×10^4, $p<0.01$ and $p<0.05$, respectively) compared with stroma-free controls (5.5×10^4 and 1.3×10^4). CD271 SP MSCs also maintained or generated significantly higher numbers of $CD34^+$ cells from $18Lin^-CD34^{+/-}$ cells (16.4×10^4 and 1.8×10^4, $p<0.01$) compared with stroma-free control and/or DN MSCs.

Interestingly, the lineage differentiation potentials of $18Lin^-CD34^{+/-}$ cells observed in the cocultures were significantly different (Table S2). The percentages of CD33, CD14 and CD11b-positive cells generated from $18Lin^-CD34^+$ cells were significantly greater than those of CD33, CD14 and CD11b-positive cells generated from $18Lin^-CD34^-$ cells ($p<0.01$) under all coculture conditions. On the contrary, the $18Lin^-CD34^-$ cells generated significantly ($p<0.01$) higher percentages of CD41-positive cells compared with $18Lin^-CD34^+$ cells under all coculture conditions. However, the absolute numbers of $CD41^+$ cells produced from one $18Lin^-CD34^{+/-}$ cell under all culture conditions were comparable. These observations suggested that the differentiation potentials of the $18Lin^-CD34^{+/-}$ cells were different, and that these two cell populations contained distinct classes of HPCs/HSCs.

Indeed, these results are consistent with the CFC capacities of both types of CB-derived $18Lin^-CD34^{+/-}$ cells. As shown in Figure S4-A, the plating efficiency (P.E.) of the $18Lin^-CD34^+$ cell fraction was approximately 75%, which contained approximately 60% to 70% CFU-GM, 20% to 30% BFU-E and <10% CFU-Mix. In contrast, the P.E. of the $18Lin^-CD34^-$ cells was approximately 65%, which contained approximately 60% BFU-E and 40% CFU-Mix (mainly consisting of erythro-megakaryocytic colonies) (CFU-EM), and CFU-GM could not be detect in this study. These findings are consistent with the results of our recent study [33, 34] showing that the highly purified $18Lin^-CD34^-$ cell fraction contains a large number of BFU-E as well as CFU-EM. In addition, we analyzed whether $18Lin^-CD34^{+/-}$ cells maintain CFC capacities after the cocultures. As shown in Figures S4-B and C, the $18Lin^-CD34^{+/-}$ cells cocultured with any type of MSCs formed significantly higher numbers of colonies, including CFU-GM, BFU-E and CFU-Mix compared with those of stroma-free cultures. Interestingly, DP MSCs supported the highest numbers of colonies derived from both cultured $18Lin^-CD34^{+/-}$ cells.

Finally, the SRC activities of cultured $18Lin^-CD34^-$ cells were assessed 20 weeks after transplantation. Equivalent numbers of cells recovered from the cocultures with or without MSCs were transplanted into NOG mice by the IBMI method (Table S3). The recipient NOG mice were sacrificed and analyzed for the presence of human $CD45^+$ cells in the BM of the left tibia (injected site) and other bones, as well as in the peripheral blood (Figures 6A-C and Table S4). Six out of the seven mice that received stroma-free cultured $CD34^-$ SRCs showed human $CD45^+$ cell engraftment in the left tibia (mean, 21.2%) and other bones (mean, 15.2%). All of the mice that received $CD34^-$ SRCs cocultured with the three MSCs showed human $CD45^+$ cell engraftment in the left tibia (mean, 55.2, 62.4 and 52.6%, respectively) and other bones (mean, 45.9, 27.0 and 38.1%, respectively). The human $CD45^+$ cell engraftment levels in the left tibiae of the mice that received cocultured $18Lin^-CD34^-$ cells were significantly higher than those of the mice that received the stroma-free control cells. Moreover, the $CD45^+$ cell engraftment levels of the other bone and peripheral blood of the mice that received $18Lin^-CD34^-$ cells cocultured with DP MSCs were significantly higher than those of the stroma-free controls. These cocultured $CD34^-$ SRCs possessed significant multi-lineage differentiation potential, including the ability to differentiate into myeloid, lymphoid (B- and T-cells), monocytic, erythroid and megakaryocytic lineages (Figure S5) as freshly isolated $CD34^-$ SRCs [33, 34]. Moreover, we analyzed whether our coculture system could produce transplantable $CD34^+CD38^-$ SRCs from $18Lin^-CD34^-$ cells. As shown in Figure S6, $18Lin^-CD34^-$ cells produced $12Lin^-CD34^+CD38^-CD45RA^-CD90^{+/-}$ cells in the cocultures with DP MSCs. Only the mice that received $CD34^+CD38^-CD90^+$ cells were repopulated with human $CD45^+$ cells with multilineage differentiation, including CD34, CD33 and CD19 cells. These results indicated that all of the MSCs established from human BM had $CD34^-$ SRC-supportive abilities, and that the DP MSCs possessed the most potent $CD34^-$ SRC-supportive ability compared with the other MSCs.

Supportive mechanisms of DP MSCs in human cord blood-derived primitive $CD34^-$ HSCs

In order to elucidate the basic supportive mechanisms of DP MSCs in human cord blood-derived primitive $CD34^-$ HSCs, we analyzed the effects of IGF-2, Wnt3a, Jagged1 and TGFβ3 on the production of $CD34^+$ cells from $18Lin^-CD34^-$ cells in the stroma-free cultures. Since the DP MSCs expressed significantly higher levels of these genes (Figure5). As shown in Figure S7, the number of cells was not significantly influenced by the presence of IGF-2, Wnt3a or Jagged1. However, TGFβ3 significantly suppressed cell proliferation compared with that observed in the IGF-2 and Jagged1-containing cultures and control culture (Figure S7A). The percentage of $CD34^+$ cells was significantly higher in the TGFβ3-containing cultures than in the other cultures (Figure S7B). Overall, the absolute number of $CD34^+$ cells produced from $18Lin^-CD34^-$ cells was significantly higher in the cultures containing IGF-2/IGFBP2 and Jagged1 compared with that noted in the control culture (Figure S7C). On the other hand, the addition of these three factors: IGF-2, Wnt3a and Jagged1, did not show any significant effects on their HSC-supporting abilities in the cocultures except in that with CD271 SP MSC (Figure S8). In separate experiments, we confirmed that the $18Lin^-CD34^{+/-}$ cells expressed unique receptors for IGF-2, Jagged1 and TGFβ3 on their surface (Figure S9). In addi-

tion, we analyzed the expression levels of these receptors on CD34$^+$CD38$^-$ cells produced in the cocultures of 18Lin$^-$CD34$^{+/-}$ cells with or without MSCs, and compared them with those of freshly isolated 18Lin$^-$CD34$^{+/-}$ cells as shown in Figure S9. The expression levels of these receptors on 12Lin$^-$CD45RA$^-$CD34$^+$CD38$^-$ cells derived from 18Lin$^-$CD34$^+$ cells in cultures were comparable to those of freshly isolated 18Lin$^-$CD34$^+$ cells. On the other hand, the expression levels of the above- mentioned receptors, except Notch 3, were upregulated compared with those of the freshly isolated 18Lin$^-$CD34$^-$ cells. However, there were no significant differences between stroma-free cultures and cocultures with MSCs. Collectively, all of these results suggest that IGF-2, Jagged1 and TGFβ3 may function as HSC-supporting factors in the stroma-free cultures.

Next, we analyzed whether contact between DP MSCs and 18Lin$^-$CD34$^{+/-}$ cells affects the supportive effects of DP MSCs on CD34$^-$ HSCs using transwell experiments. As shown in Figure S10, the 18Lin$^-$CD34$^{+/-}$ cells yielded almost equivalent amounts of CD34$^+$ cells in the cocultures with DP MSCs, consistent with the data presented in Figure S3. However, in the presence of the transwell, the above mentioned CD34$^{+/-}$ HSC-supportive effects were almost abrogated. These results clearly demonstrate that the direct adhesion of DP MSCs with CD34$^{+/-}$ SRCs is important for the HSC-supportive function of DP MSCs.

Functional characterization of single DP cell-derived MSCs

As shown in Figure 2B, the frequency of CFU-F in the DP MSCs was about 1/6. Therefore, we further analyzed the cellular characteristics of the DP MSCs at the single clone level in order to elucidate whether they were still heterogeneous. First, to confirm the CFU-F frequency of the DP fraction at the single clone level, single DP cells were sorted onto 96-well plates and cultured for 13 days, and then were assessed for their CFU-F frequency. The frequencies of single DP cell-derived CFU-F were 1/6.4 and 1/5.3 (Figure 7A), which were similar to that of the bulk DP cell fraction. In addition, we succeeded in obtaining 33 single cell derived-DP MSCs.

Next, we tested the proliferation potentials of these single cell-derived DP MSCs. The single cell-derived DP MSCs were cultured for 40 days and passaged once or twice during this period. Then, these DP MSCs were collected, and the numbers of cells were counted. We found that 16/33 of the single cell-derived DP MSCs stopped their growth after the first or second passages. The numbers of remaining single cell-derived DP MSCs (17/33) on day 40 are presented in Figure 7B. The median number was 6.8 x 10^5 cells. The single DP cells that showed the highest or lowest proliferation ability yielded to 30.5 x 10^5 or 0.4 x 10^5 cells, respectively. Therefore, the single cell-derived DP MSCs showed a wide range of growth potential.

We then evaluated the osteogenic and adipogenic differentiation potential of the single cell-derived DP MSCs using three clones. Our results demonstrated that all three clones were unable to differentiate into adipocytes (Figure 7C, third and bottom rows), similar to the DP MSCs established from bulk DP cells. Unexpectedly, the osteogenic differentiation potential of these three clones was heterogeneous (Figure 7C, top and second rows).

Then, we analyzed the surface marker expression levels of another six single cell-derived DP MSCs. All six clones expressed CD90 and SSEA-4, but did not express CD34, CD41, CD45, or CD56. Interestingly, all of these clones also had downregulated the surface expression of CD271 (Figure 7D), like the bulk cell derived-DP MSC. Therefore, the surface marker expression levels of these single cell-derived DP MSCs were indistinguishable from each other after the cultures.

Furthermore, we tested the supportive effects of single cell-derived DP MSCs on CB-derived 18Lin$^-$CD34$^{+/-}$ cells *in vitro*. The cocultures were performed in the same way as described in Figure S3. The CB-derived 18Lin$^-$CD34$^{+/-}$ cells were seeded onto the feeders of three single cell-derived DP MSCs. After seven days of coculture, the fold-increases in the total number of cells and the percentages of CD34$^+$ cells in CD45$^+$ cells were analyzed by FCM. As shown in Figure 7E, the fold-increases of 18Lin$^-$CD34$^{+/-}$ cells were approximately 100- to 150-fold, and 60- to 90-fold, respectively. There were no remarkable differences between the fold increases of each of the single cell-derived DP MSC feeders. The percentages of CD34$^+$ cells maintained/generated from 18Lin$^-$CD34$^{+/-}$ cells were approximately 25% in the cocultures with two DP MSC feeders, and approximately 10% in the coculture with clone 7. All of these results suggest that even single cell-derived DP MSCs are still functionally heterogeneous.

DISCUSSION

As a standard technique, human BM-derived MSCs are isolated/identified as fibroblastic adherent cells in culture [11]. However, it is still uncertain whether the MSCs isolated by this technique consist of a homogeneous cell population or not. In this study, we tried to clarify this important issue. As described in the Results section, we discovered that the human MSCs isolated from the BM Lin$^-$CD45$^-$ fraction contain at least two types of cell populations. One is MSCs, which show osteo-chondro-adipogenic differentiation potential, and were isolated from the CD271$^{+/-}$SSEA-4$^-$ fractions (DN or CD271 SP MSCs). Another is MSCs, which show osteo-chondrogenic differentiation potential when isolated from the CD271$^+$SSEA-4$^+$ fraction (DP MSCs). Interestingly, the surface marker expressions of established MSCs after four passages *in vitro* became indistinguishable between these MSCs (Figure 3). Therefore, it seemed to be difficult to isolate DP MSCs from other MSCs after *in vitro* expansion culture.

The gene expression profiles of transcriptional factors required for *in vitro* differentiation in the MSCs were

then analyzed using qRT-PCR (Figure 5). We found that the expression levels of *RUNX2* and *SP7*, which were essential for the osteogenic differentiation [38, 39], of DP MSCs were significantly higher than those of the DN or CD271 SP MSCs. The expression level of *SOX9*, which was expressed in the osteo-chondroprogenitor [40], of DP MSCs was not higher than that of the DN and CD271 SP MSCs. The gene expression of *PPARG*, which is a master regulator for adipogenic differentiation [41], was not detected in any MSCs at the steady state (data not shown). Hence, it is unclear from the present data why the DP MSC could not be induced to differentiate into adipocytes. However, the DP MSCs expressed significantly higher levels of *FOXC1*, which was reported to be preferentially expressed in the adipo-osteogenic progenitor CAR cells essential for HSPC maintenance [36]. It was also clearly demonstrated that *FOXC1* inhibited adipogenic processes in CAR progenitors [36]. Therefore, high expression of *FOXC1* in the DP MSCs may have been related to their lack of adipogenic differentiation potential.

Recently, a number of investigators reported that the many types of stromal cells support primitive HSCs in the mouse BM niche [6-10]. However, it has not been fully elucidated whether human BM-derived MSCs support primitive human HSCs or not. Therefore, we evaluated the ability of the three established MSCs to support human HPCs/HSCs using highly purified 18Lin$^-$CD34$^{+/-}$ cells, which contained primitive HPCs/HSCs, as target populations [33, 34]. As previously reported [37, 38], human CB-derived CD34$^-$ HSCs are more primitive HSCs within the human HSC hierarchy compared with CD34$^+$ HSCs. Therefore, in this study, we used CD34$^-$ SRCs as a source of human primitive HSC in order to investigate the HSC-supportive effects of the three established MSCs.

As shown in Figure 6, all of the MSCs showed comparable abilities to support human CD34$^-$ SRCs when the human CD45$^+$ cell engraftment levels were evaluated in the left tibiae (injected site) of mice (Figure 6A). However, in the other bones, only the mice that received 18Lin$^-$CD34$^-$ cells cocultured with DP MSCs showed significantly higher human cell repopulation compared with that of the stroma-free control (Figure 6B). In addition, the mice that received CD34$^-$ SRCs cocultured with DP MSCs showed significantly higher percentages of human CD45$^+$ cell engraftment in the peripheral blood, compared with the stroma-free control (Figure 6C). Collectively, these results imply that when CD34$^-$ SRCs are cocultured with DP MSCs, they might acquire higher migration and homing abilities. These results also demonstrate that DP MSCs possess a higher HSC-supportive ability compared with other MSCs.

It was previously reported that human MSCs also expressed nestin and supported human CD34$^+$CD38$^-$ hematopoietic cells through membrane-bound SDF-1 [37]. Therefore, we analyzed the gene expression level of nestin in these established MSCs. As we expected, the DP MSCs expressed a significantly higher level of nestin mRNA than did the other MSCs (Figure 5). To clarify the mechanisms underlying the SRC-supportive abilities of MSCs, we next analyzed the gene expression profiles of well-characterized HSC-supportive genes [1, 36, 37, 42-46] by qRT-PCR. We found that the DP MSCs more strongly expressed *IGF2*, *WNT3A*, *JAG1*, *ANGPT1*, *TGFB3* and *CXCL12* compared with DN and CD271 SP MSCs (Figure 5). These results suggest that the higher SRC-supportive ability of DP MSCs may correlate with their higher expression of HSC-supportive genes. As described in the Results section, IGF-2, Wnt3a and Jagged1 exerted HSC-supportive effects in the stroma-free cultures to some degree (Figure S7). However, the direct adhesion of CD34$^{+/-}$ HSCs with DP MSCs appeared to be more important for the support/maintenance of primitive human CD34$^{+/-}$ HSCs (Figure S10). Therefore, in order to understand the mechanisms underlying the ability of the MSCs to support SRC, we analyzed the expression of adhesion molecules and integrins (CD29, CD49d, CD49e and CD49f) before and after the cocultures (Figure S9). As shown in Figure S9, 12Lin$^-$CD45RA$^-$ CD34$^+$CD38$^-$ cells produced from 18Lin$^-$CD34$^{+/-}$ cells in the cocultures expressed almost comparable levels of these integrins. Therefore, further studies are needed to identify as yet undermined adhesion molecules or signal transducing receptors that may play a pivotal role in supporting HSCs. As also shown in Figure 5, three established MSCs showed different gene expression profiles, suggesting that the mechanisms of three MSCs for supporting SRC may be different from each other. In addition, the DP MSCs expressed a significantly higher level of *FOXC1*, which was recently identified as a critical regulator of HSPC niche formation by CAR cells [36]. These results may suggest that the DP MSCs are human homologues of mouse CAR cells.

From another point of view, it was recently reported that adipocytes function as a negative regulator of the BM microenvironment [47]. Namely, HPCs/HSCs were reduced in frequency in the adipocyte-rich vertebrae of the mouse tail relative to the adipocyte-free vertebrae of the thorax. Moreover, the relative frequency of KLS (CD45$^+$Lin$^-$kit$^+$Sca-1$^+$) cells was lower in the cells cocultured with adipocytic OP9 stromal cells compared to those cocultured with undifferentiated OP9 stromal cells [47]. Adipocytes and osteocytes originate from MSCs within the BM, where both cells have a reciprocal relationship [47, 48]. Therefore, it is interesting that DP MSCs lacking adipogenic differentiation potential exhibited better CD34$^-$ SRC-supportive abilities compared with other MSCs having trilineage differentiation potential. Collectively, the DP MSCs and other BM-MSCs may play different roles in the human HSC niche.

CONCLUSION

MSCs established from the BM Lin$^-$CD45$^-$ cell fraction contain at least two populations. One is DP MSCs that have a restricted osteo-chondrogenic differentiation potential, while the others are DN and CD271 SP MSCs,

which can differentiate into all three lineages. These two populations may differ not only in their differentiation capacity, but also in their ability to support primitive HSCs. Based on our findings, we cannot fully elucidate whether the three MSCs have hierarchical differences as do the HSCs, or whether these MSCs are distinct populations. Therefore, it is important to clarify the functional heterogeneity of these established MSCs, in order to better understand the hierarchy of human MSCs.

Acknowledgments

This work was supported by Grants-in-Aid for Scientific Research C (Grant Nos. 21591251 and 24591432) from the Ministry of Education, Culture, Sports, Science and Technology (MEXT) of Japan; a grant from the Science Frontier Program of the MEXT; a grant of A-STEP (Adaptable & Seamless Technology Transfer Program through Target-driven R&D) Feasibility Study (FS) Stage (Exploratory Research type) from the Japan Science and Technology Agency (JST) (Grant No.AS231Z03109G); a grant from the Strategic Research Base Development Program for Private Universities from the MEXT; the MEXT-Supported Program for the Strategic Research Foundation at Private Universities; a grant from the Promotion and Mutual Aid Corporation for Private Schools of Japan; a grant from the Japan Leukemia Research Foundation; a grant from the Mitsubishi Pharma Research Foundation; a grant from the Takeda Science Foundation; a grant from the Terumo Life Science Foundation and a grant from SENSHIN Medical Research Foundation. All these grants were given to Yo.So. This work was also supported by Grants-in-Aid for Young Scientists (B) (Grant Nos. 24790984 and 26860741) from the Japan Society for the Promotion of Science; a grant from Kansai Medical University (Research grant D1); a grant from the Science Research Promotion Fund and a grant from the Takeda Science Foundation given to Y.M. The authors are grateful to the Japanese Red Cross Kinki Cord Blood Bank for providing the samples used in this study.

Author Contributions

Y.M.: conception and design, financial support, provision of study material, collection and/or assembly of data, data analysis and interpretation, manuscript writing; R.N., K.S., H.K., M.T., T.F., Y.U.: and Y.S.: provision of study material, collection and/or assembly of data; H.A.: statistical analysis; M.I., H.O.: T.T.: and M.H.: provision of study material; Y.S.: conception and design, financial support, administrative support, data analysis and interpretation, manuscript writing, and final approval of manuscript.

References

1 Mercier FE, Ragu C, Scadden DT. The bone marrow at the crossroads of blood and immunity. Nat Rev Immunol 2012;12:49-60.
2 Morrison SJ, Scadden DT. The bone marrow niche for haematopoietic stem cells. Nature 2014;505:327-334.
3 Calvi LM, Adams GB, Weibrecht KW et al. Osteoblastic cells regulate the haematopoietic stem cell niche. Nature 2003;425:841-846.
4 Zhang J, Niu C, Ye L et al. Identification of the haematopoietic stem cell niche and control of the niche size. Nature 2003;425836-841.
5 Kiel MJ, Yilmaz OH, Iwashita T et al. SLAM family receptors distinguish hematopoietic stem and progenitor cells and reveal endothelial niches for stem cells. Cell 2005;121:1109-1121.
6 Ding L, Saunders TL, Enikolopov G et al. Endotherial and perivascular cells maintain haematopoietic stem cells. Nature 2012;481:457-462.
7 Sugiyama T, Kohara H, Noda M et al. Maintenance of the hematopoietic stem cell pool by CXCL12-CXCR4 chemokine signaling in bone marrow stromal cell niches. Immunity 2006;25:977-988.
8 Omatsu Y, Sugiyama T, Kohara H et al. The essential functions of adipo-osteogenic progenitors as the hematopoietic stem and progenitor cell niche. Immunity 2010;33:387-399.
9 Mendez-Ferrer S, Michurina TV, Ferraro F et al. Mesenchymal and haematopoietic stem cells form a unique bone marrow niche. Nature 2010;466:829-834.
10 Greenbaum A, Hsu YM, Day RB et al. CXCL12 in early mesenchymal progenitors is required for haematopoietic stem-cell maintenance. Natute 2013;495:227-230.
11 Pittenger MF, Mackay AM, Beck SC et al. Multilineage potential of adult human mesenchymal stem cells. Science 1999;284:143-147.
12 Morikawa S, Mabuchi Y, Niibe K et al. Development of mesenchymal stem cells partly originate from the neural crest. Biochem Biophys Res Commun 2009;379:1114-1119.
13 Muraglia A, Cancedda R, Quarto R. Clonal mesenchymal progenitors from human bone marrow differentiate in vitro according to a hierarchical model. J Cell Sci 2000;113:1161-1166.
14 Jones EA, Kinsey SE, English A et al. Isolation and characterization of bone marrow multipotential mesenchymal progenitor cells. Arthritis Rheum 2002;46:3349-3360.
15 Simmons PJ, Torok-Storb B. Identification of stromal cell precursors in human bone marrow by a novel monoclonal antibody, STRO-1. Blood 1991;78:55-62.
16 Sacchetti B, Funari A, Michienzi S et al. Self-renewing osteoprogenitors in bone marrow sinusoids can organize a hematopoietic microenvironment. Cell 2007;131:324-336.
17 Mabuchi Y, Morikawa S, Harada S et al. LNGFR^{+}THY-1^{+}VCAM-1^{hi+} cells reveal functionally distinct subpopulations in mesenchymal stem cells. Stem Cell Rep 2013;1:152-165.
18 Quirici N, Soligo D, Bossolasco P et al. Isolation of bone marrow mesenchymal stem cells by anti-nerve growth factor receptor antibodies. Exp Hematol 2002;30:783-791.
19 Tormin A, Li O, Brune JC et al. CD146 expression on primary nonhematopoietic bone marrow stem cells is correlated with in situ localization. Blood 2011;117:5067-5077.
20 Gang EJ, Bosnakovski D, Figueiredo CA et al. SSEA-4 identifies mesenchymal stem cells from bone marrow. Blood 2007;109:1743-1751.
21 Battula VL, Treml S, Bareiss PM et al. Isolation of functionally distinct mesenchymal stem cell subsets using antibodies against CD56, CD271, and mesenchymal stem cell antigen-1. Haematologica 2009;94:173-184.
22 Pinho S, Lacombe J, Hanoun M et al. PDGFRα and CD51 mark human Nestin^{+} sphere-forming mesenchymal stem cells capable of hematopoietic progenitpor cell expansion. J Exp Med 2013;210:1351-1367.

23 Ogawa M. Differentiation and proliferation of hematopoietic stem cells. Blood 1993;81:2844-2853.
24 Morrison SJ, Shah NM, Anderson DJ. Regulatory mechanisms in stem cell biology. Cell 1997;88:287-298.
25 Bryder D, Rossi DJ, Weissman IL. Hematopoietic stem cells: the paradigmatic tissue-specific stem cell. Am J Pathol 2006;169:338-346.
26 Dick JE. Normal and leukemic human stem cells assayed in SCID mice. Semin Immunol 1996;8:197-206.
27 Larochelle A, Vormoor J, Hanenberg H et al. Identification of primitive human hematopoietic cells capable of repopulating NOD/SCID mouse bone marrow: Implications for gene therapy. Nat Med 1996;2:1329-1337.
28 Wang JCY, Doedens M, Dick JE. Primitive human hematopoietic cells are enriched in cord blood compared with adult bone marrow or mobilized peripheral blood as measured by the quantitative in vivo SCID-repopulating cell assay. Blood 1997;89:3919-3924.
29 Hogan CJ, Shpall EJ, Keller G. Differential long-term and multilineage engraftment potential from subfractions of human CD34⁺ cord blood cells transplanted into NOD/SCID mice. Proc Natl Acad Sci U S A 2002;99:413-418.
30 Wang J, Kimura T, Asada R et al. SCID-repopulating cell activity of human cord blood-derived CD34⁻ cells assured by intra-bone marrow injection. Blood 2003;101:2924-2931.
31 Kimura T, Asada R, Wang J et al. Identification of long-term repopulating potential of human cord blood-derived CD34⁻flt3⁻ severe combined immunodeficiency-repopulating cells by intra-bone marrow injection. Stem Cells 2007;25:1348-1355.
32 Kimura T, Matsuoka Y, Murakami M et al. *In vivo dynamics of human cord blood-derived CD34⁻ SCID-repopulating cells using intra-bone marrow injection.* Leukemia 2010;24:162-168.
33 Ishii M, Matsuoka Y, Sasaki Y et al. Development of a high-resolution purification method for precise functional characterization of primitive human cord blood-derived CD34-negative SCID-repopulating cells. Exp Hematol 2011;39:203-213.
34 Takahashi M, Matsuoka Y, Keisuke S et al. CD133 is a positive marker for a distinct class of primitive human cord blood derived CD34-negative hematopoietic stem cell. Leukemia 2014;28:1308-1315.
35 Sonoda Y. Immunophenotype and functional characteristics of human primitive CD34-negative hematopoietic stem cells: the significance of the intra-bone marrow injection. J Autoimmun 2008;30:136-144.
36 Omatsu Y, Seike M, Sugiyama T et al. Foxc1 is a critical regulator of haematopoietic stem/progenitor cell niche formation. Nature 2014;508:536-540.
37 Schajnovitz A, Itkin T, D'Uva G et al. CXCL12 secretion by bone marrow stromal cells is dependent on cell contact and mediated by connexin-43 and connexin-45 gap junctions. Nat Immunol 2011;12:391-398.
38 Komori T, Yagi H, Nomura S et al. Targeted disruption of Cbfa1 results in a complete lack of bone formation owing to maturational arrest of osteoblasts. Cell 1997;89:755-764.
39 Nakashima K, Zhou X, Kunkel G et al. The novel zinc finger-containing transcription factor osterix is required for osteoblast differentiation and bone formation. Cell 2002;108:17-29.
40 Akiyama H, Kim JE, Nakashima K et al. Osteo-chondroprogenitor cells are derived from Sox9 expressing precursors. Proc Natl Acad Sci U S A 2005;102:14665-14670.
41 Tontonoz P, Hu E, Spiegelman BM. Stimulation of adipogenesis in fibroblasts by PPARγ 2, a lipid-activated transcription factor. Cell 1994;79:1147-1156.
42 Arai F, Hirao A, Ohmura M et al. Tie2/angiopoietin-1 signaling regulates hematopoietic stem cell quiescence in the bone marrow niche. Cell 2004;118:149-161.
43 Batard P, Monier MN, Fortunel N et al. TGF-β1 maintains hematopoietic immaturity by a reversible negative control of cell cycle and induces CD34 antigen up-modulation. J Cell Sci 2000;113:383-390.
44 Willert K, Brown JD, Danenberg E et al. Wnt proteins are lipid-modified and can act as stem cell growth factors. Nature 2003;423:448-452.
45 Yamazaki S, Iwama A, Takayanagi S et al. TGF-β as a candidate bone marrow niche signal to induce hematopoietic stem cell hibernation. Blood 2009;113:1250-1256.
46 Zhang CC, Lodish HF. Insulin-like growth factor 2 expressed in a novel fetal liver cell population is a growth factor for hematopoietic stem cells. Blood 2004;103:2513-2521.
47 Naveiras O, Nardi V, Wenzel PL et al. Bone-marrow adipocytes as negative regulators of the hematopoietic microenviroment. Nature 2009;460:259-263.
48 Nuttall ME, Gimble JM. Controlling the balance between osteoblastogenesis and adipogenesis and the consequent therapeutic implications. Curr Opin Pharmacol 2004;4:209-204.

See www.StemCells.com for supporting information available online. STEM CELLS; *00:000–000*

